Title

Release of Matrix Tension Modulates Invasive Phenotype Differently in Breast Cancer than in Mammary Epithelial Cells

Author

Contreras, Ryne Lucas

Publication Date

2019

Peer reviewed|Thesis/dissertation

UNIVERSITY OF CALIFORNIA SAN DIEGO

Release of Matrix Tension Modulates Invasive Phenotype Differently in Breast Cancer than in Mammary Epithelial Cells

A thesis submitted in partial satisfaction of the requirements for the degree Master of Science

in

Bioengineering

by

Ryne Lucas Contreras

Committee in charge:

Professor Stephanie Fraley, Chair
Professor Adam Engler
Professor Jing Yang

2019

The Thesis of Ryne Lucas Contreras is approved and it is acceptable in quality and form for publication on microfilm and electronically:

Chair

University of California San Diego

2019

TABLE OF CONTENTS

LIST OF FIGURES

LIST OF GRAPHS

ACKNOWLEDGEMENTS

I would like to thank Professor Stephanie Fraley for taking a chance on me, providing me with the freedom to pursue hypotheses of my own observation, and providing guidance on how to interpret my findings in a productive way to inspire further research. Her insight and experience were vital for helping me appreciate less than desirable results and provide new perspective when I was lost in the weeds.

I would also like to thank all the members of the Fraley Lab, whose openness to lend knowledge and provide perspective was crucial for supporting my research development. I have never been part of a learning environment this talented and also equally willing share their share their knowledge. For that, I am truly grateful.

Finally, I would like to thank my family for all their love and support over these two plus years. It is important for me to put my current work in perspective with the rest of my life and remember that it is not my life. They were instrumental in providing me with breaks needed to recognize and appreciate this.

VITA

2013 Bachelor of Science, Biomedical Engineering, California Polytechnic State University San Luis Obispo, San Luis Obispo

2019 Master of Science, Bioengineering, University of California San Diego

ABSTRACT OF THESIS

Release of Matrix Tension Modulates Invasive Phenotype Differently in Breast Cancer than in Mammary Epithelial Cells

by

Ryne Lucas Contreras

Master of Science in Bioengineering

University of California San Diego, 2019

Professor Stephanie Fraley, Chair

Cell migration is thought to be driven by interactions with the surrounding environment. Utilizing the core four biophysical features including adhesion, contractility, degradation, and actin cytoskeletal polymerization, cells interrogate their environment and use sensory feedback to promote proliferation or migration. Collagen I, an essential component of the stroma has been implicated in inducing migratory behavior in both normal and cancer cells, suggesting that the microenvironment plays a key role in directing cell fate. Additionally, matrix tension is thought to be a promoter of contractile force generation and invasion in normal cells. Recent studies were able to induce invasive behavior in MCF10A normal mammary epithelial cells by implanting them in a collagen I rich environment. However, release of matrix tension promoted conversion of cells to a non-invasive phenotype. Since we've demonstrated persistent collective invasion of

MDA-MB-231 cancer cells is promoted in low attachment environments, I hypothesized that cancer cells would be less sensitive to the effect of matrix tension release. Comparison of tension release in normal cells vs cancer cells demonstrated significant, but less distinctive shift in distribution towards the non-invasive spheroid phenotype in cancer. Uniquely, low matrix tension conditions promoted proliferation in structures independent of invasiveness. Additionally, invasive network phenotypes acquired pseudo-normal morphology including capacity for lumen formation. Investigation of potential cell-ECM and cell-cell interaction driving this behavior suggested that increased cell-cell adhesion and contractility induced intercellular tension regulates invasive behavior and may stimulate proliferation increases. Finally, calcium mediated adhesion was found to play an important role in structure stability.

CHAPTER 1: INTRODUCTION

1.1. Content Introduction

Cancer is a complex and challenging disease that will affect over 1.7 million new patients this year. [1] Although the damaging effects of cancer are well known, what is less understood is roughly 90% of all cancer related deaths can be attributed to metastasis. [2] During metastasis, cancer cells from the primary tumor site develop invasive potential and invade through tissue to vasculature or lymphatic ducts, where they intravasate into circulation, before eventually extravasating at the site of distant metastasis. There is a lack of understanding of how and what stimulates cancer cells to begin invasion through tissue.

Two hallmarks of cancer are its proliferative and migratory capabilities. To grow and expand into new tissue, cancer utilizes enhanced degradation, adhesion, actin cytoskeleton polymerization, and contractile processes to manipulate and remodel its environment. Normal cells utilize these biophysical features in a regulated manner to maintain tensional homeostasis which is critical for survival and migration on cell, tissue, organ, and organism scales. Current research suggests that contractile forces are needed to manipulate the surrounding matrix and that matrix tension in turn promotes migration in normal cells. Loss of matrix tension is associated with a reduced ability to grip the matrix and apply traction forces needed to migrate. In development, heterogenous tension in the developing embryo helps drive the formation of the different germ layers and later, complex tissue geometries contained within each organism. [3] During normal tissue maintenance, cells proactively remodel their environment to minimize stress development, and in the event of injury or disease, wound healing processes promotes cell migration to the injury and synthesis of new tissue to cover the wound and restore force balance to the surrounding tissue architecture. [4] In cancer, tensional balance is often dysregulated, leading to extremely dense tumor cell masses with core necrosis and the deposition of extensive collagen I (COL I) rich ECM which helps facilitate their migration and

eventually metastasis. At the genesis of breast cancer metastasis, aberrant breast cancer cells are thought to invade out of collagen type IV (COL IV) and laminin rich basement membrane into COL I rich stroma. Cellular contact with COL I, a key structural component of most tissue ECM, has been implicated in driving both cancer and normal epithelial cells to invade. [5,6,7]

Invasion can be divided into 3 major forms including single cell ameboid blebbing, mesenchymal, and collective migration. Recent evidence suggests that collective migration is the preferred invasion mode among cancer cells, allowing for intercellular heterogeneity (i.e. leader-follower cells, etc.) to better facilitate migration, intravasation, immune system suppression, and extravasation to the secondary tumor site. [6,8] This migration mode is not unique to cancer cells, and is used in more regulated segments during embryonic development, wound closure, and in particular during mammary ductal invasion into the mammary fat pad. In cancer, the signaling pathways that promote invasion from primary tumor to distant metastatic sites are not well understood and lack the *in vitro* and *in vivo* models to study them. Building an understanding of the dynamic connections between cancer cells, adjacent cells, and their microenvironment will be vital to understanding the trigger points in the metastatic cascade.

Cells have keen potential to sense changes in their physical environment, including ability to sense matrix rigidity as low as 100-200 Pa and sense thicknesses on the order of 10's of um [9,10]. Cell populations existing within a tissue receive frequent force inputs from surrounding ECM and adjacent cells, then apply stimulus dependent mechanotransduction. This is referred to as outside-in signaling. Alternatively, cells can actively probe their immediate environment and react via inside-out signaling. To facilitate the transmission of mechanosignals, cells commonly connect to the ECM using integrins at the center of focal adhesions (FA), and to adjacent cells using cadherin homophilic binding at the center of adherens junctions (AJ). [11,12] Downstream signaling from FA complexes and AJ can mediate migration, invasion, polarization, proliferation, dormancy, and differentiation. Additionally, many epithelial cell types regulate

tension homeostasis to support cell polarization and luminal patency in acinar and ductal structures. [13] During cancer growth and invasion however, mechanotransduction pathways are hijacked and dysregulated to stimulate uncontrolled growth, survival, and invasion, which often results in a lack of cell polarity and cell layer organization. Despite the unorganized appearance of primary tumors, many invasive cancer cells are capable of downregulating these processes to form pseudo-normal morphology at sites of distant metastasis, which aids pathologists in discovering the origin of the metastasizing tissue. [14,15]

In vitro, researchers have also been able to induce cancer cells to adopt pseudo-normal morphology and behavior, i.e. proliferation and migration normalization, by placing cancer cells in non-aberrant microenvironments, co-culturing them with normal cells, or providing certain environmental stimuli. [16,17,1,18] For example, invasive triple negative MDA-MB-231 breast cancer cells injected at a ratio of 1:50 with mouse epithelial cells into a cleared mouse mammary fat pad were able to regenerate chimeric mammary ductal growths capable of secretory function including the production of milk protein alpha lactalbumin. [1] This suggests cancer cells retain memory of their unmutated cellular lineage and fully differentiated identity. Moreover, normal cells have been induced to display aberrant behavior when placed in cancer environments. The current body of evidence suggests that plasticity exists in normal as well as in cancer cells and that the extracellular matrix (ECM) can play a key role in directing cell fate.

COL I is a major component of mammary ECM, and is used extensively in breast cancer research. Researchers leverage its invasive promoting characteristics to study aberrant epithelial cell behavior and cancer progression. For example, Carey, et al. 2017, showed that COL I induces invasive behavior in noninvasive MCF10A immortalized breast epithelial cells. [5] Interestingly, this aberrant migration behavior can be reverted by floating the 3D collagen environment, i.e. detaching it from its container. It is thought that floating effectively releases intra-matrix tension and that this tension is required for protrusive signaling that promotes

invasion. The goal of my thesis work was to test whether this hypothesis holds true for cancerous epithelial cells.

1.2. 3D COL I Hydrogel System

Previous research by our lab demonstrated the ability of our 3D COL I hydrogel system to induce both cancerous MDA-MB-231 (MDA) and non-cancerous MCF10A breast epithelial cells to undergo collective migration. However, our studies also showed that these cells were not strongly adhered to the COL I environment, which seems to contradict the hypothesis that cell-ECM tension promotes invasion. Our hydrogel system forms 2 major collectively migrating phenotypes including invasive network structures and non invasive spheroidal structures.

1.3. Hydrogel System Nomenclature

- Attached- Gel polymerizes in a 48 wellplate and becomes attached to the sides and bottom.
- Floated- Gel polymerizes in a 48 wellplate and becomes attached to the sides and bottom. Gel is gently removed with a thin instrument around the perimeter, scooped out of the dish and placed in a larger 24 well plate dish filled with media. Gel does not reattach to bottom or side at any future point.

Chapter 2: Methods

2.1. Cell Culture:

MDA-MB-231 cells were provided by Adam Engler (UCSD Bioengineering). MCF10A cells were purchased from (ATCC, Manassas, VA). MDA-MB-231 cell line was cultured in high glucose Dulbecco's Modified Eagle's Medium supplemented with 10% (v/v) fetal bovine serum (FBS, Corning, Corning, NY) and 0.1% gentamicin (Gibco Thermofisher, Waltham, MA). MCF10A cell line was cultured in Dulbecco's Modified Eagle's Medium: Nutrient Mixture F12 supplemented with 5% Horse Serum (Invitrogen, Waltham, MA), 0.02% 100ug/ml stock EGF (Peprotech, Rocky Hill, NJ), 0.05% of 1mg/ml stock Hydrocortisone (Sigma Aldrich, St. Louis, MO), 0.01% 1mg/ml stock Cholera Toxin (Sigma Aldrich), 10mg/ml stock Insulin (Sigma Aldrich), and 1% gentamicin (Gibco Thermofisher). All cells were maintained at 37 °C and 5% CO2 in a humidified environment during culture and imaging. The cells were passaged every 2–3 days.

2.2. 3D Culture in COL I Matrix

Cell embedded 3D collagen matrices were prepared by mixing trypsinized cells suspended in culture medium and 10X reconstitution buffer, 1:1 (v/v), with either low density 2.5mg/ml (LD) or high density 6mg/ml (HD) concentration of soluble rat tail type I collagen in acetic acid (Corning, Corning, NY). A proportionate volume of 1 M NaOH was used to neutralize collagen solution pH for each concentration (pH 7.0, 10-20 µl 1 M NaOH). Selectively, macromolecular crowding agent PEG (8000 kDa, Sigma, St. Louis, MO), was added to the formulation of 2.5mg gels at a final concentration of 10mg/ml to induce high density architecture (small fibers) in low density gels (LDSF) as described by our previous work. [M2] Gels were polymerized at 37°C in a humidified incubator.

2.3. Antibodies and Inhibitors:

2.3.1. 3D Immunostaining Antibodies

COL IV alpha 1 (Novus Biologicals, Centennial, CO, 1:200) , LAM 5ÓÓ y2 chain (Millipore Sigma, Burlington, MA, 1:200), YAP (D8H1X) XP(R) (Cell Signaling Technologies, Danvers, MA, 1:250), E-cadherin (Protein Tech, Rosemount, IL, 1:200), E-cadherin (Abcam, Cambridge MA, 1:50) EpCAM D48KR XP(R) (Cell Signaling Technologies, 1:100) , Muc-1 (Abcam, 1:200), Ki67 (Cell Signaling Technologies, 1:400), DAPI (Thermofisher Scientific, 1:1000), Alexa Fluor 488 Phalloidin (Invitrogen, 1:40)

2.3.2. Western Blotting Antibodies

Primaries: P-FAK tyr 397 (Invitrogen, 1:1000), alpha tubulin (Thermofisher Scientific, Waltham, MA 1:5000), GAPDH (Cell Signaling Technologies, 1:5000)

Secondaries: Alexa Fluor 405 (Rabbit host), Alexa Fluor 488 (Mouse host), Alexa Fluor 546 (Mouse or Rabbit host) (Thermofisher Scientific, 1:500), HRP (Mouse or Rabbit host) (Cell Signaling, Technologies, 1:5000)

2.3.3. Inhibitors

Y27632 ROCK I, II inhibitor (Tocris Biosciences, Bristol, UK, 10µM), Myosin Light Chain Kinase (MLCK) inhibitor M-7 (Tocris Biosciences, 20µM), Calcium chelating agent EDTA (Thermofisher Scientific, 2-4mM)

2.4. Immunofluorescence and Microscopy

2.4.1. Immunofluorescence

At experiment endpoint, gel media is removed and gel is transferred to 24 well plate if not currently incubating in one (i.e. attached condition). Gel is rinsed with PBS, then fixed with 4% Paraformaldehyde solution (Electron Microscopy Sciences, Hatfield, PA) for 30 min. After sufficient washing, gels are incubated in blocking solution with or without Tritionx100 (Fisher Bioreagents) depending on the staining application for 1 day with agitation at 4C. Blocking solution is removed and rinsed thoroughly. All further incubations described are followed by

thorough rinsing. Primary antibody is incubated for 2 days with agitation at 4C. Secondary antibody is incubated for 1 day. Gels are stored in PBS in a dark container until imaging.

2.4.2. Epifluorescent/Brightfield (BF) Imaging

Nikon TI Eclipse Microscope (Nikon Instruments, Minato, Tokyo, Japan) was used for BF and Fluorescent imaging. 10X dry objective was used for BF structure distribution images and stacks. 40X oil immersion objective was used for individual structure BF and fluorescent imaging and stacks.

2.4.3. Confocal Imaging

Confocal images were acquired using upright or inverted microscope systems. Individual experiments (i.e. YAP signal for each hydrogel condition was acquired with the same microscopy system) were completed on the same microscope for consistency. First, an upright Leica SP5 confocal microscope (Leica Microsystems, Buffalo Grove, IL) was equipped with a 20X water immersion objective. Next an inverted Leica SP8 confocal microscope (Leica Microsystems) was used for confocal and confocal reflection imaging using a 40X water immersion objective. Last the inverted Zeiss LSM 880 Confocal with Fast Airy Scan (Zeiss, Pleasanton, CA) was equipped with 20X water immersion objective. For confocal reflection imaging on the Leica SP8 confocal microscope, the sample was excited at 488 nm and reflected light was collected without an emission filter. Non reflection confocal imaging was performed using the excitation laser and filter to accommodate the fluorophore(s) of interest. Image processing including measurements, overlays, merging, and image processing were performed using FIJI (NIH, Rockville, MD).

2.5 Western Blotting

Cells were embedded in collagen hydrogels and grown up for 7 days. Cells were removed from culture plate, placed in a 2ml protein lo-bind vial, and washed with ice cold PBS. Fresh PBS was added, then gel was centrifuged at 1500 Xg for 5 min. Next PBS was removed and cells were lysed with Pierce Lysis IP Buffer (Thermofisher Scientific) was added in

equal volume to the gel volume. 100X Halt protease and phosphatase inhibitor cocktails (Thermofisher Scientific) were added at working concentrations to prevent protein degradation prior to incubation of the solution for 15 minutes on ice. Sufficient Bolt LDS 4X sample buffer (Thermofisher Scientific) and 10X DTT (Thermofisher Scientific) was added to the lysis solution reach working concentrations. The formulation was briefly vortexed, then incubated for 1hr with vortexing repeated every 15 min. Samples were then denatured via incubation at 95C for 5 min. Samples were loaded for gel electrophoresis, ran, and transferred for 17.5hrs at 40V to PVDF membranes (0.2 or 0.45µm pore size). Blots were then blocked, immunostained with the primary antibody of interest and an HRP linked secondary, and developed with Clarity Western Blotting ECL Substrate (Bio-Rad, Hercules, CA) for visualization. Protein of interest band values were normalized to either alpha tubulin or GAPDH depending on the host animal of the protein of interest, then relative protein content was compared.

2.6. Image Quantification

2.6.1. Cell Counts

Using FIJI's (NIH) cell counter plugin, DAPI signals within the z stacks of structures were counted to quantify the number of cells per structure. Care was taken to not double count individual DAPI signals present over multiple slices.

2.6.2. YAP Nuclear to Cytoplasmic Ratio

In FIJI (NIH), Confocal images with DAPI and YAP channels were split. DAPI masks were created by binarizing the raw DAPI channel, filling any holes, and segmenting close nuclei using the adjustable watershed plugin. Using the DAPI masks as ROIs, mean intensity value and area measurements were rerouted to the YAP channel. Additionally, individual masks were selected, 0.25 µm bands were drawn around the perimeter, and mean intensity and area was calculated using a custom macro. $YAP_{N/C}$ was calculated by dividing mean nuclear intensity by mean ring (cytoplasmic) intensity.

2.7. Mycoplasma Testing

New cell lines and existing cell lines (periodically) were tested for Mycoplasma contamination. Plate reading assay was performed according to LONZA Mycoalert® Mycoplasma Detection Kit (Lonza, Basel, Switzerland) protocol. Any positive samples would be double confirmed with a PCR based protocol adapted from [19], using the genus specific components listed below:

Custom primers: Sense primer GPO3 (5′ GGGAGCAAACAGGATTAGATACCCT3′), Antisense primer MGSO (5′TGCACCATCTGTCACTCTGTTAACCTC3′) as first described in [19] for mycoplasma species detection before performing experiments. A custom oligo of the 16S conserved region in bacteria modeled from Mycoplasma Hyrohindis served as the positive control:

Forward Complement:

AGCGTGGGGAGCAAACAGGATTAGATACCCTGGTAGTCCACGCCGTAAACGATGA
TCATTAGTTGGTGGAATAATTTCACTAACGCAGCTAACGCGTTAAATGATCCGCCTG
AGTAGTATGCTCGCAAGAGTGAAACTTAAAGGAATTGACGGGAACCCGCACAAGCG
GTGGAGCATGTGGTTTAATTTGAAGATACGCGTAGAACCTTACCCACTCTTGACATC
TTCTGCAAAGCTATAGAGATATAGTGGAGGTTAACAGAGTGACAGATGGTGCATGG
TTGT

Reverse Compliment:

ACAACCATGCACCATCTGTCACTCTGTTAACCTCCACTATATCTCTATAGCTTTGCA
GAAGATGTCAAGAGTGGGTAAGGTTCTACGCGTATCTTCAAATTAAACCACATGCTC
CACCGCTTGTGCGGGTTCCCGTCAATTCCTTTAAGTTTCACTCTTGCGAGCATACTA
CTCAGGCGGATCATTTAACGCGTTAGCTGCGTTAGTGAAATTATTCCACCAACTAAT
GATCATCGTTTACGGCGTGGACTACCAGGGTATCTAATCCTGTTTGCTCCCCACGC
T(Integrated DNA Technologies, San Diego, CA)

2.8 Statistics

All statistical analyses with the exception of power were performed with Graphpad Prism 5 (San Diego, CA). Power analyses were performed using G*Power 3.1.9.2 (Düsseldorf, Germany). Unless specified elsewhere, all statistical measures utilized α and β of 0.05. Effect size was generated using Cohen's d statistic. *A priori* determination of sample size used power $(1- \beta) = 0.95$. *Post hoc* power verification confirmed power ≥ 0.95. Findings of significance were demarcated as follows: * $p<0.05$, ** $p<0.01$, *** $p<0.001$. Further instructions are provided *pro re nata* in figure description.

CHAPTER 3: RESULTS

3.1 Model Translation and Comparison

3.1.1. Effect of Matrix Density on Invasive Phenotype

Carey et al. utilized a 1.5mg/ml collagen 1 hydrogel system as their model. These gels produced small aggregates of MCF10A cells which displayed stellate behavior in attached conditions, while when floated displayed far more round morphology and a reduction in protrusions over the 4-day culture period. In our gel system, we have found that collectively migration is promoted in higher density (HD) 6mg/ml concentrations of COL I. To bridge this gap in density, I utilized previous work from our lab where we were able to decouple stiffness from density using PEG mediated macromolecular crowding in low density (LD) 2.5mg gel during polymerization of our hydrogel. Previous work has demonstrated macromolecular crowding during collagen polymerization creates similar small fiber architecture which is sufficient to promote collective migration. [20] Utilizing the low density small fiber (LDSF) gels, I was able to more directly recapitulate their gel conditions.

I measured the extent to which MDA cells took on invasive or non-invasive phenotypes in floated versus attached LDSF COL I matrices after 7 days and compared this to the behavior of MCF10A cells as a model of normal cell behavior. For MCF10A cells, release of matrix tension immediately following polymerization (F_0) resulted in a distinct -6.38-fold shift in the ratio of invasive to non-invasive structures (networks:spheroids ratio) in favor of spheroids, whereas MDA structures experienced a -1.23-fold shift. (Graphs 1,2) I next hypothesized that the effect of floatation was density dependent, suggesting that cells in HD hydrogel would not be sensitive to tension release. Following matrix release, HD hydrogel structures demonstrated -1.10-fold shift in favor of spheroids. (Graph 3) Excitingly, MDA cells demonstrate similar, albeit less distinct, reduction in invasive phenotype irrespective of COL I density.

Graph 1. MCF10A LDSF floated hydrogel structures display substantial fold change in favor of the non-invasive spheroid phenotype. Distribution of network and spheroid phenotype in attached and floated COL I hydrogels. Fold changes in networks with respect to attached hydrogels are -6.38 and -10.50 for F_0 and F_24 respectively. N= 1 hydrogel. Took 3 representative z stacks of 800µm thick. About n=200 total structures counted in each z-stack. Statistical significance is tested by ANOVA and reported as p<0.001, ***; p<0.01, **; p<0.05, *.

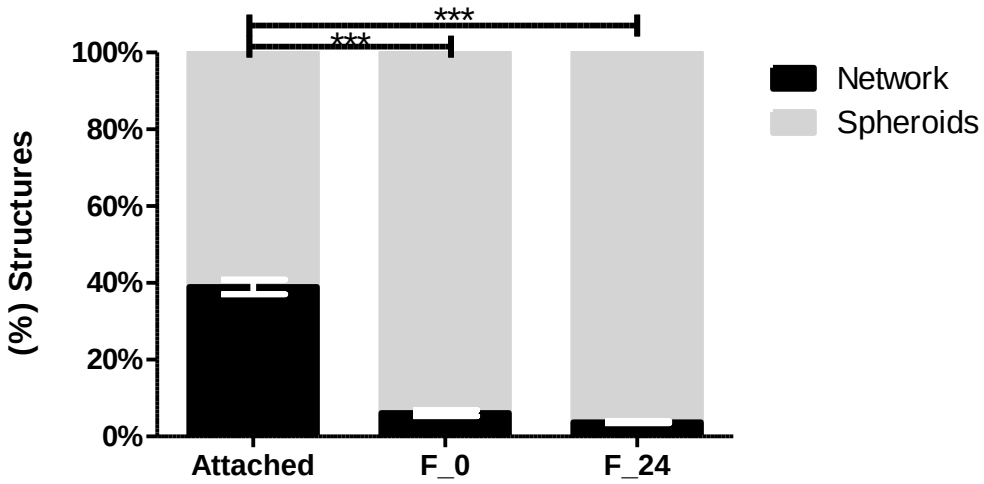

Graph 2. MDA LDSF floated hydrogel structures display substantial fold change in favor of the non-invasive spheroid phenotype. Distribution of network and spheroid phenotype in attached and floated COL I hydrogels. Fold changes in networks with respect to attached hydrogels are -1.23 and -1.30 for F_0 and F_24 respectively. N= 1 hydrogel. Took 3 representative z stacks of 800µm thick. About n=200 total structures counted in each z-stack. Statistical significance is tested by ANOVA and reported as p<0.001, ***; p<0.01, **; p<0.05, *.

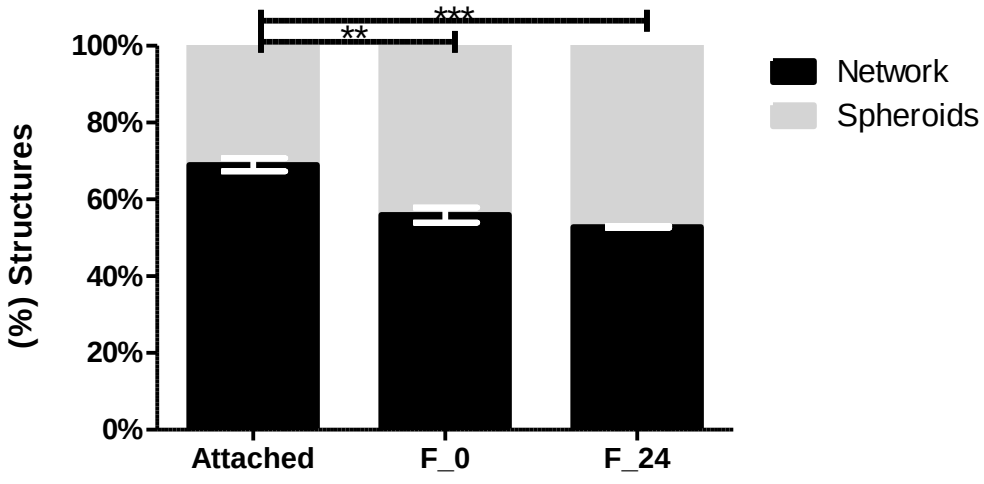

Graph 3. MDA HD floated hydrogel structures display substantial fold change in favor of the non-invasive spheroid phenotype. Distribution of network and spheroid phenotype in attached and floated COL I hydrogels. Fold changes in networks with respect to attached hydrogels are -1.10 and -1.14 for F_0 and F_24 respectively. N= 1 hydrogel. Took 3 representative z stacks of 800µm thick. About n=200 total structures counted in each z-stack. Statistical significance is tested by ANOVA and reported as p<0.001, ***; p<0.01, **; p<0.05, *.

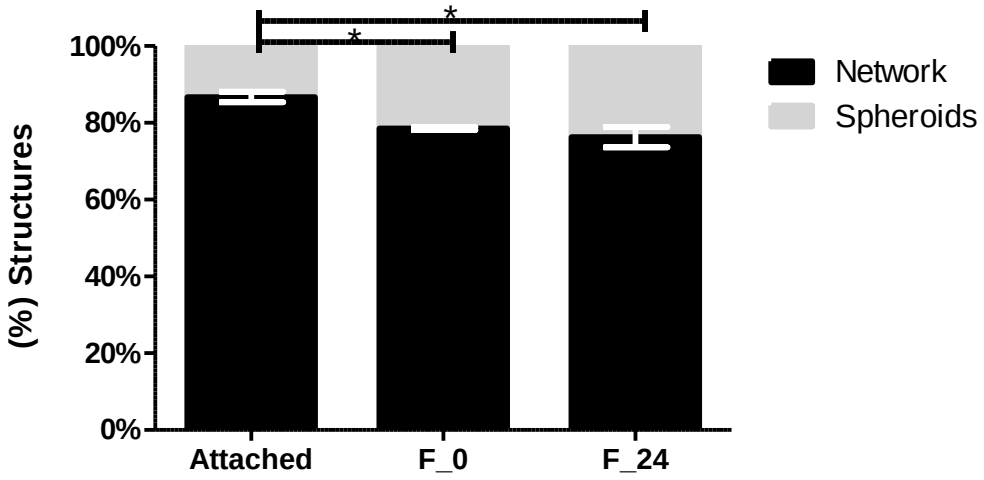

3.1.2. Effect of Persistent Invasion Niche on Invasive Phenotype

Previous work demonstrated that cells placed in our low adhesion matrices began to invade more persistently after the first division (~16-20 hrs), and this behavior was consistent for the remainder of time in 3D culture. I hypothesized that allowing cells to establish the persistent invasion niche would inhibit future efforts to reduce suppress invasive phenotype, i.e. floating after the first division. When HD and LDSF hydrogels were released from the well plate after 24hrs (F_24) i.e. after the first division, MDA structures experienced a -1.14- and -1.30-fold shift, respectively, in favor of spheroids. (Graphs 2, 3) These ratios were very similar to what was observed in F_0 hydrogels. However, when I released a LDSF hydrogel containing MCF10As, structures experienced fold shift of -10.50, nearly double the fold shift experienced by F_0 hydrogels. (Graph 1) Yet biologically the distribution change is similar. Since both normal and cancer cells experienced significant reductions in invasive phenotype, but cancer cells demonstrated lower sensitivity to matrix release, I was interested in what other morphological changes could be observed among the two cell types.

3.1.3. Morphology Characterization

Interestingly, I observed that floated MCF10A hydrogels spheroids had significantly greater diameters, but there was no significant difference in spheroid widths (Figure 1 and Graph 4, 5) Similarly, MDA floated hydrogel spheroids also had significantly greater diameters. (Figure 2 and Graph 6). Invasive networks remained the most prevalent phenotype in MDA floated hydrogels, and they displayed increased width, but not length. (Figure 2, Graphs 7, 8) MCF10A networks showed the capacity for increased width, but overall the population width was not significantly larger than the attached condition. (Figure 1)

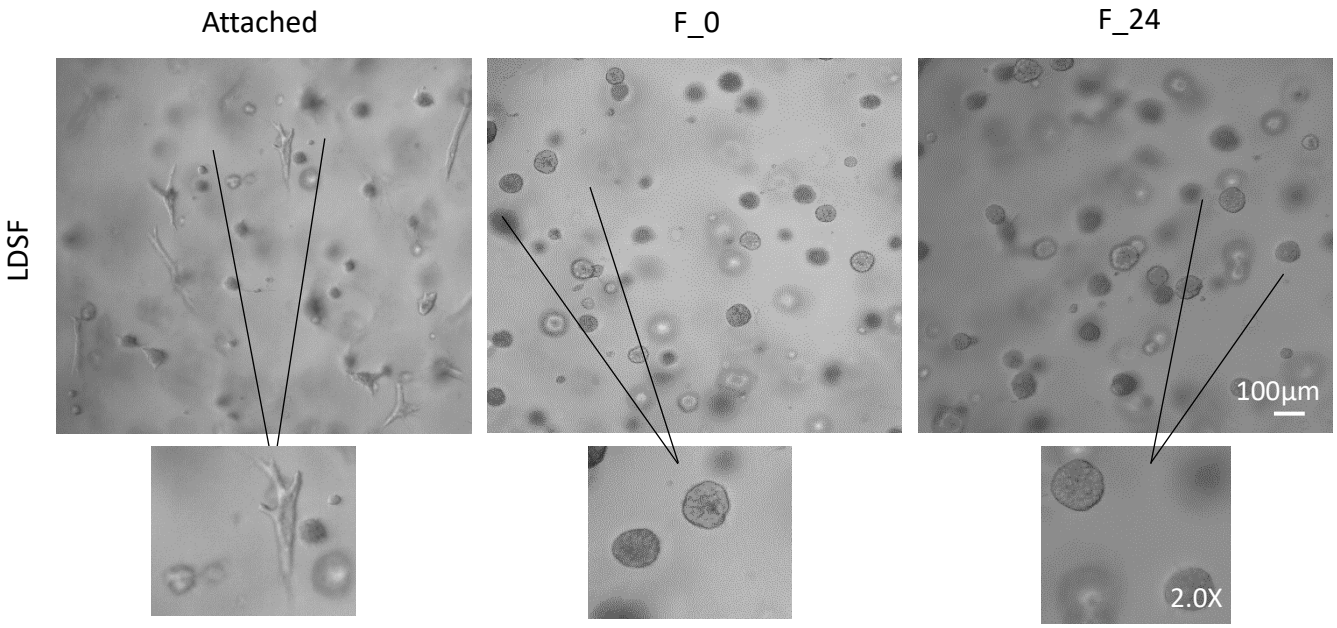

Figure 1. Brightfield images of MCF10A LDSF attached and floated hydrogel conditions. Spheroids are noticeably larger in diameter. Although not frequently present, cells still form networks in floated hydrogel conditions. 2x zoom images show representative morphology.

Graph 4. MCF10A LDSF floated hydrogel spheroids have significantly larger diameters than attached hydrogel spheroids. N= 20 spheroids measured per hydrogel condition. Statistical significance is tested by ANOVA and reported as p<0.001, ***; p<0.01, **; p<0.05, *.

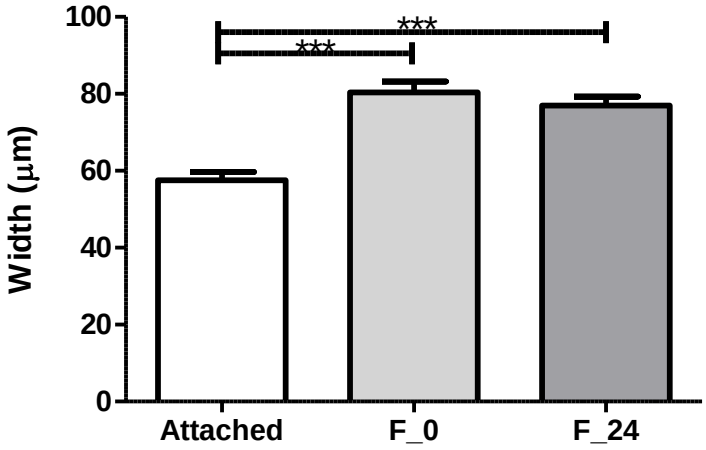

Graph 5. MCF10A LDSF floated hydrogel networks do not have significantly larger widths than attached hydrogel networks. N= 20 networks measured per hydrogel condition. Statistical significance is tested by ANOVA and reported as p<0.001, ***; p<0.01, **; p<0.05, *.

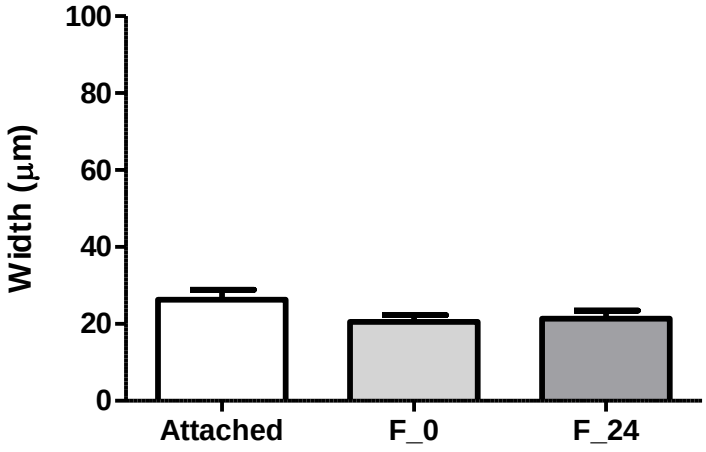

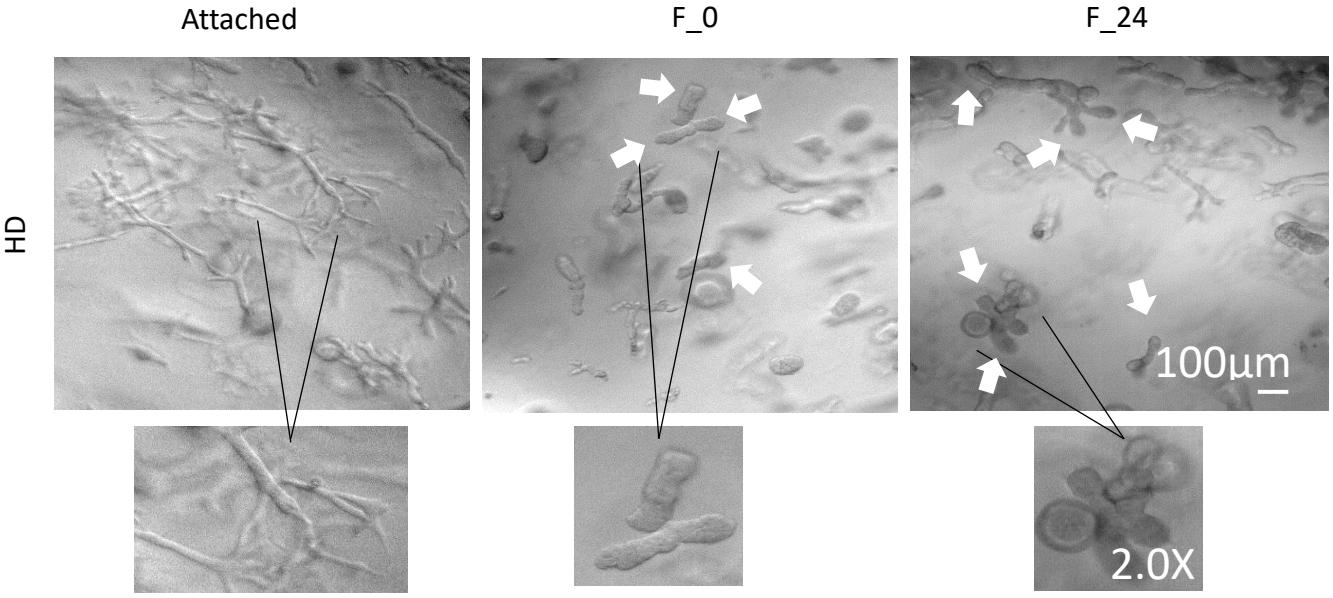

Figure 2. Brightfield images of MDA HD attached and floated hydrogel conditions. In floated hydrogel's networks widths are noticeably thicker and spheroids diameter are noticeably larger. Additionally, Networks display bulb ends as indicated by arrows. 2x zoom images show representative morphology.

Graph 6. MDA HD floated hydrogel spheroids have significantly larger diameters than attached hydrogel spheroids. N= 20 networks measured per hydrogel condition. Statistical significance is tested by ANOVA and reported as p<0.001, ***; p<0.01, **; p<0.05, *.

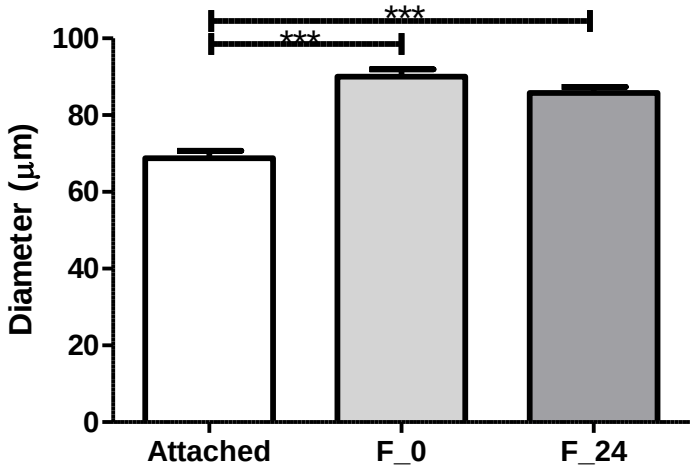

Graph 7. MDA HD floated hydrogel networks have significantly longer widths than attached hydrogel networks. N= 20 networks measured per hydrogel condition. Statistical significance is tested by ANOVA and reported as p<0.001, ***; p<0.01, **; p<0.05, *.

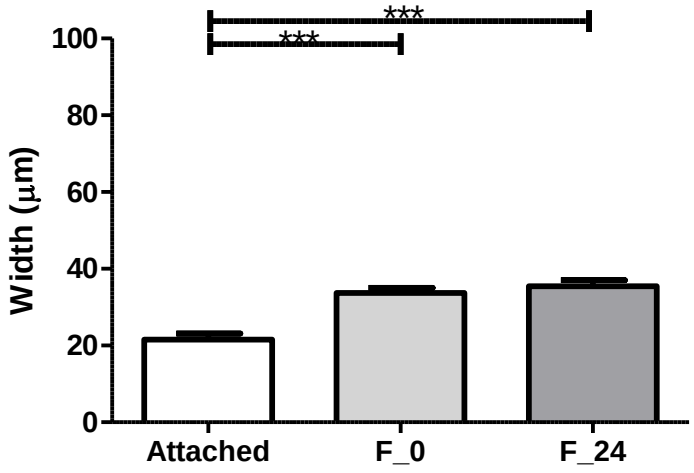

Graph 8. MDA HD floated hydrogel networks are not significantly longer than attached hydrogel networks. N= 20 networks measured per hydrogel condition. Statistical significance is tested by ANOVA and reported as p<0.001, ***; p<0.01, **; p<0.05, *.

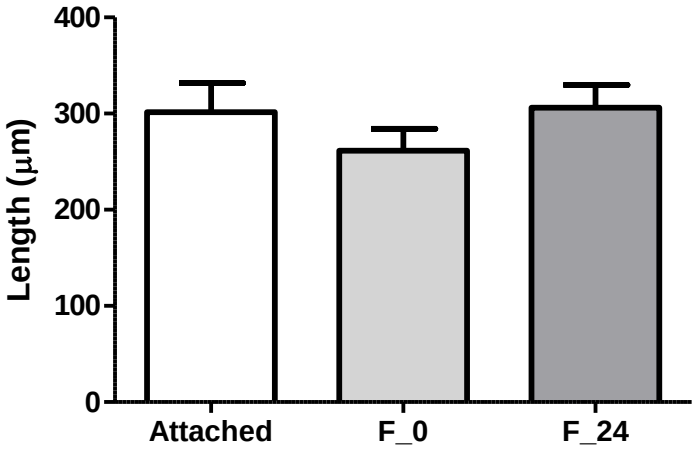

Considering length did not change significantly, but width did, I wondered if width directly correlated with cell increase within the MDA networks. Pearson's correlation analysis demonstrated that width was strongly correlated with cell count r(30) = .78, p<0.0001, in HD

hydrogel network structures. (Graph 7, 9, 10) Significantly larger spheroid diameters matched had also significantly larger cell counts. (Graph 6, 11) Significant increased proliferation in floated conditions was not shown in Carey et al. and demonstrates a unique feature of floatation with our hydrogel system. Together, with the shifts in invasive phenotype, these results suggest that proliferation is upregulated in normal and cancerous cells under low matrix tension independent of invasiveness.

Graph 9. MDA network width is highly correlated with its total cell count. N= 10 networks widths measured and number of cells counted per hydrogel condition. Pearson's correlation: r(28)= .78, p<0.0001.

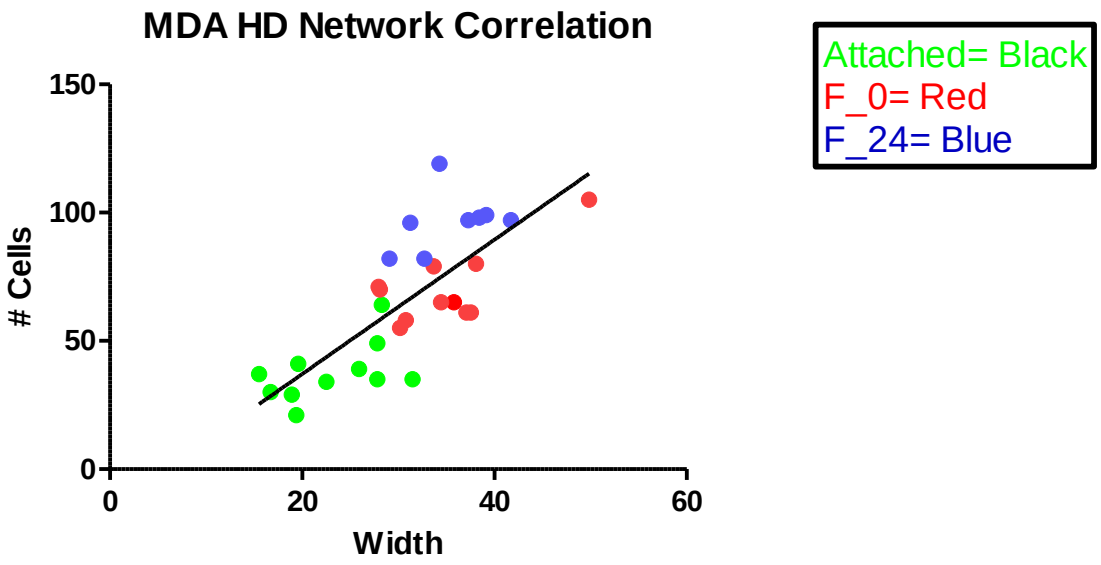

Graph 10. MDA HD floated hydrogel networks contain significantly more cells than attached hydrogel networks. N= 10 networks measured per hydrogel condition. Statistical significance is tested by ANOVA and reported as p<0.001, ***; p<0.01, **; p<0.05, *.

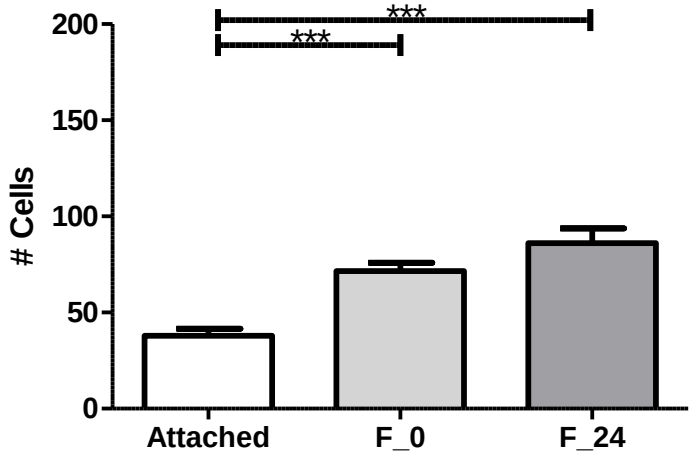

Graph 11. MDA HD floated hydrogel spheroids contain significantly more cells than attached hydrogel spheroids. N= 10 networks measured per hydrogel condition. Statistical significance is tested by ANOVA and reported as p<0.001, ***; p<0.01, **; p<0.05, *.

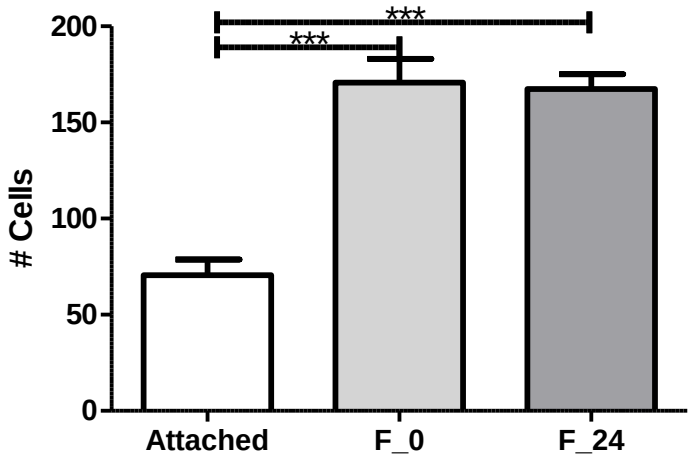

Phenotypically, invasive MDA networks displayed bulbous ends reminiscent of normal mammary terminal lobular ductal units. (Figure 1) Inspired by the increased network widths and bulb ends, we wondered if these floated hydrogel structures were also hollow. As illustrated using DAPI and or phalloidin staining in Figure 3 a small amount of floated network and

spheroid structures demonstrated partial luminal patency. Lumens were identified by persistent alignment of cells bordering a cell free gap. Since we expected proliferating networks to invade further with increased proliferation, but instead noticed new patterns of cell structure organization reminiscent of normal mammary development, we were curious how cells were able to support this new geometry.

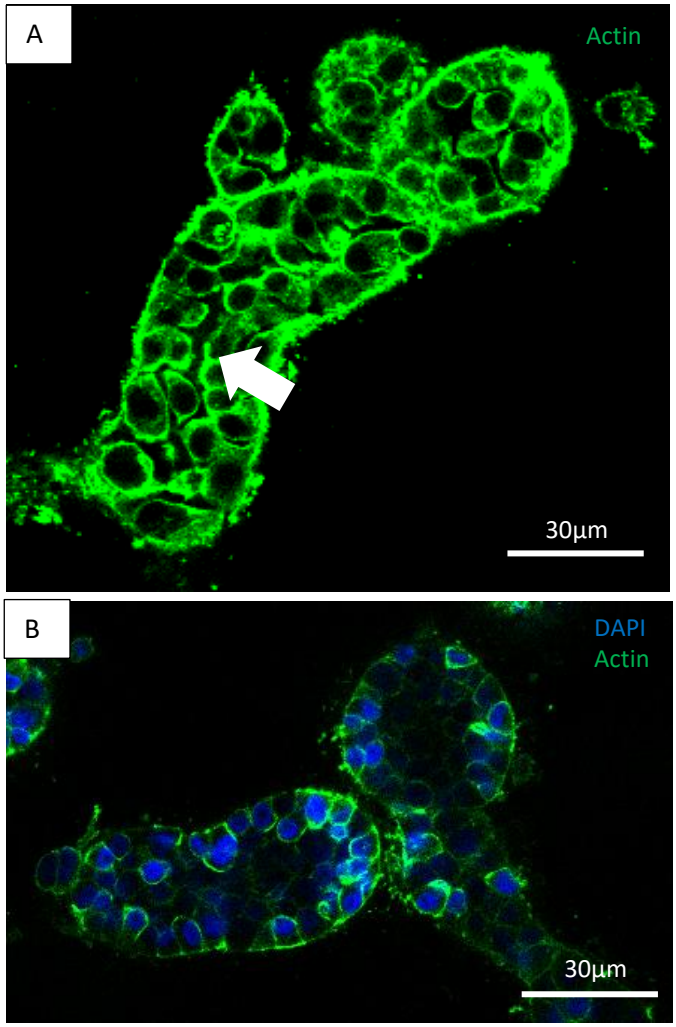

Figure 3. Confocal images of MDA lumen formation floated hydrogel networks and spheroids. A: Phalloidin stain to visualize lumen formation. Arrow points towards middle of lumen. B: DAPI/Phalloidin stain to visualize hollow network (left) and spheroid (right)

3.2 Building an Understanding of the Cell-ECM and Cell-Cell Interactions

3.2.1. Nascent ECM Deposition:

Normal mammary structures deposit basement membrane ECM proteins to support their environment. I hypothesized that floated structures, displaying more normal behavior, promoted expression of nascent deposition to support migration in low attachment. Surprisingly, collagen 4 (COL4A1) and laminin 5 (LAMC2) which have been shown to be heavily implicated in creating this secure connection, demonstrated deposition in both invasive and non invasive structures. (Figure 4)

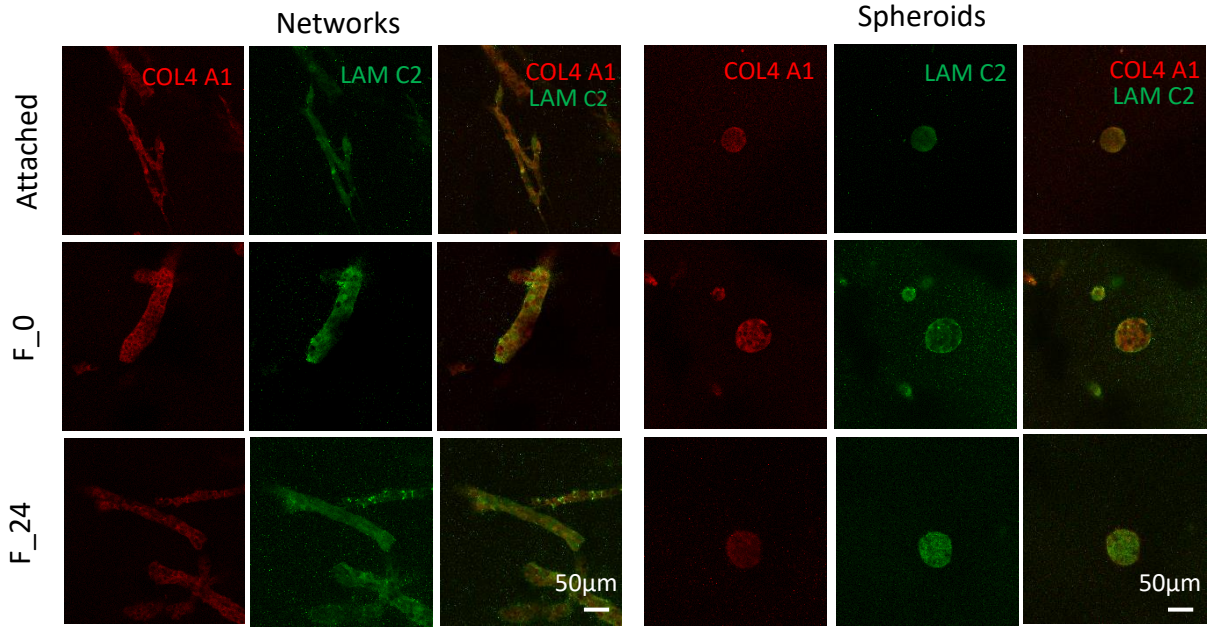

Figure 4. Confocal images of MDA nascent ECM deposition in attached and floated hydrogel conditions. Networks and spheroids regardless of hydrogel condition demonstrate internal expression and external deposition.

Basement membrane ECM deposition is largely considered a program for non-invasive cells, yet here invasive cells also utilize it, suggesting expanded utility of endogenous matrix proteins during collective invasion and metastasis. However, previous knockdown (KD) of either COL4A1 or LAMC2 did not prevent collective migration, although these KD cells were not tested

in floated conditions to demonstrate potential morphological benefits. [21] Therefore, we next hypothesized that cell-cell interactions, rather than cell-ECM interactions, supported both invasive and non-invasive structure formation.

3.2.2. FAK Activation at Cell-Cell Junctions

Adherens junctions (AJ), the main cell-cell adhesion protein complexes, transmit most mechanosignaling between cells. FAK serves as a scaffolding and signaling protein at focal adhesions, but can also be recruited as a signaling protein through interactions with AJ proteins alpha and beta catenin. Activated FAK (pFAK) has been implemented in several downstream proliferative signaling cascades including SRC, MAPK, and ERK. [22] We hypothesized that pFAK levels would be increased if cell-cell interactions were enhanced by floating the COL I matrices. Indeed, a 1.4-2.3 fold increase in pFAK among floated hydrogels relative to attached hydrogels demonstrated a potential role for this interaction. (Graph 12)

Graph 12. MDA floated hydrogel structures promote increased pFAK expression relative to attached hydrogel structures. N= 1 protein sample per hydrogel condition.

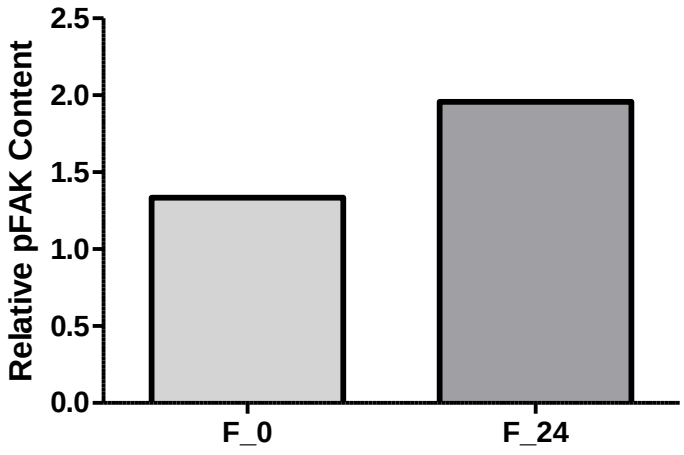

The presence of FAK suggested greater number of cell-cell adhesions were developing in floated structures. FAK is a mechanosensitive signaling protein that can be activated through tension. The HIPPO pathway has also been observed to be inhibited when tension develops at AJs. Inhibition of the HIPPO pathway can promote downstream proliferative and morphogenesis upregulations. [23,24] Therefore, I hypothesized that HIPPO pathway inhibition is upregulated in floated structures.

3.2.3. Cell-Cell Tension Mediated YAP Nuclear Localization

YAP nuclear localization is a common indicator of HIPPO pathway inhibition and cell cycle progression. I measured individual cell nuclear to cytoplasmic ratio ($YAP_{N/C}$) n average it among hydrogel conditions to get a preliminary idea of YAP signaling across the different hydrogel conditions Interestingly, cells within floated hydrogels did not demonstrate higher average $YAP_{N/C}$ than in attached hydrogels at day 7. (Graph 13)

Graph 13. Individual MDA $YAP_{N/C}$ is not different among attached and floated hydrogel structures. About N=25 cells measured per representative confocal slice from z stack of a structure. 2 networks and 2 spheroids measured per hydrogel condition. Individual cell ratios averaged from each set of 4 structures per hydrogel condition. Statistical significance is tested by ANOVA and reported as p<0.001, ***; p<0.01, **; p<0.05, *.

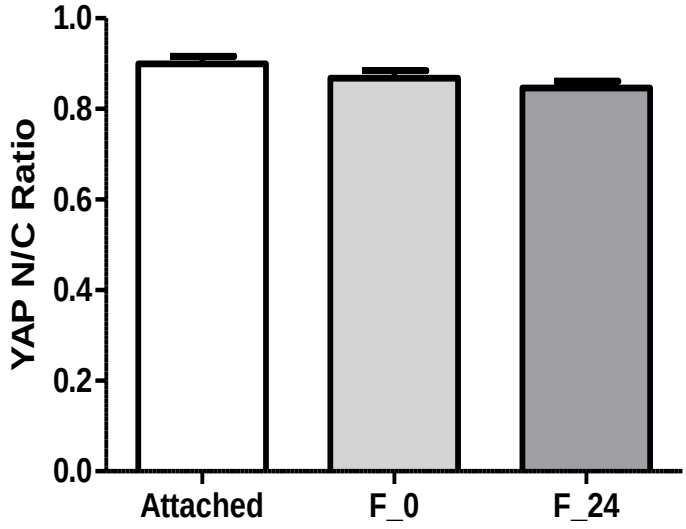

However, Ki67 immunostaining for proliferation suggested that elevated proliferation rate (19-28%) occurs earlier during development (~day 5) compared to day 7 (1-9%). (Graphs 14-17) Divergence in size (width, diameter) and morphology between attached and floated structures is also observed at day 5, suggesting this is an important morphological time range to study YAP nuclear translocation.

Graph 14. Day 7 proliferation in MDA network structures. N=5 networks per hydrogel condition. Statistical significance is tested by ANOVA and reported as p<0.001, ***; p<0.01, **; p<0.05, *.

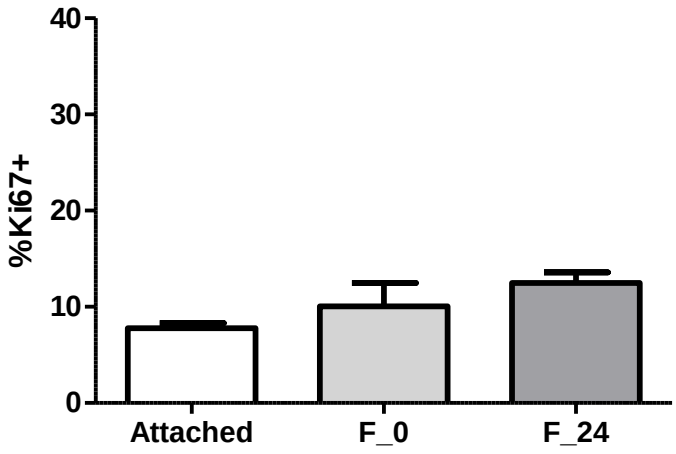

Graph 15. Day 7 proliferation in MDA spheroid structures. N=5 spheroids per hydrogel condition. Statistical significance is tested by ANOVA and reported as p<0.001, ***; p<0.01, **; p<0.05, *.

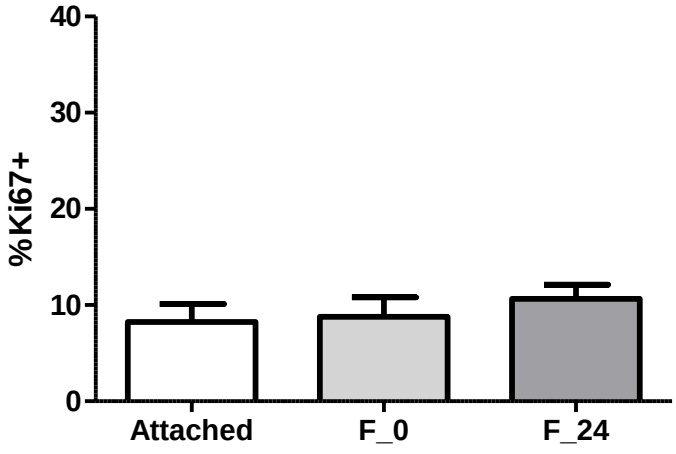

Graph 16. Day 5 proliferation in MDA network structures. Proliferation is 2-3 times higher at day 5 than day 7. N=5 networks per hydrogel condition. Statistical significance is tested by ANOVA and reported as p<0.001, ***; p<0.01, **; p<0.05, *.

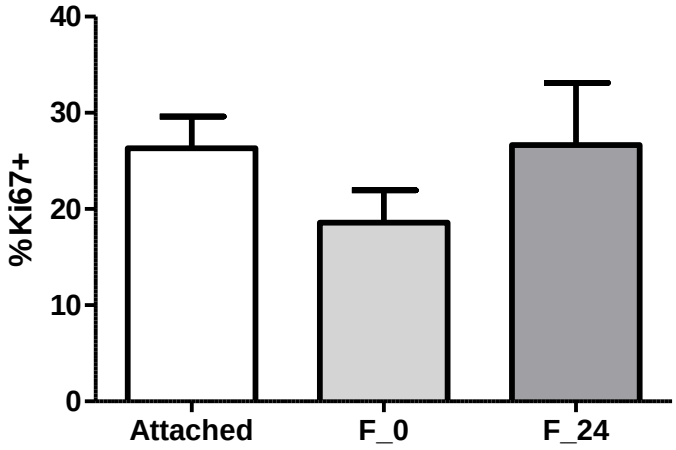

Graph 17. Day 5 proliferation in MDA spheroid structures. Proliferation is 2-3 times higher at day 5 spheroids than day 7 spheroids. N=5 networks per hydrogel condition. Statistical significance is tested by ANOVA and reported as p<0.001, ***; p<0.01, **; p<0.05, *.

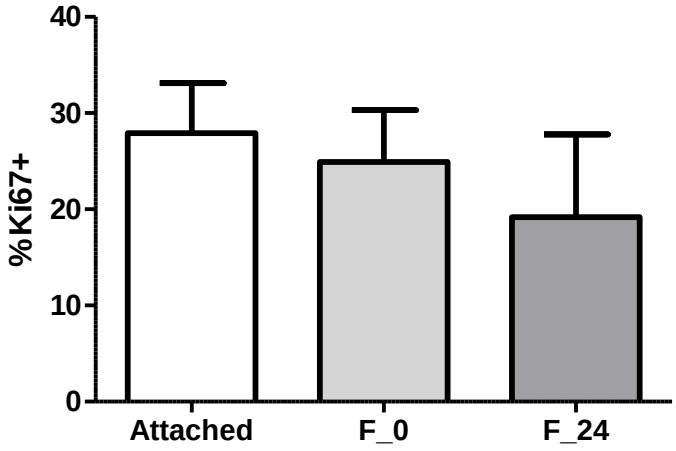

Despite not identifying an expected increase in $YAP_{N/C}$, I also observed that Individual cells in structures displayed heterogeneous cytoplasmic YAP signal, including higher expression in the more peripheral layers of spheroids and floated networks. (Figure 5) Nonetheless, there was no distinguishable pattern of elevated $YAP_{N/C}$ perimeter cells. (Figure 6) Further characterization of the temporal window of signaling for each condition will be important for future studies. To

eliminate the time requirement, I next looked to inhibit contractility consistently overtime to see if tension at cell-cell contacts is important for morphological development.

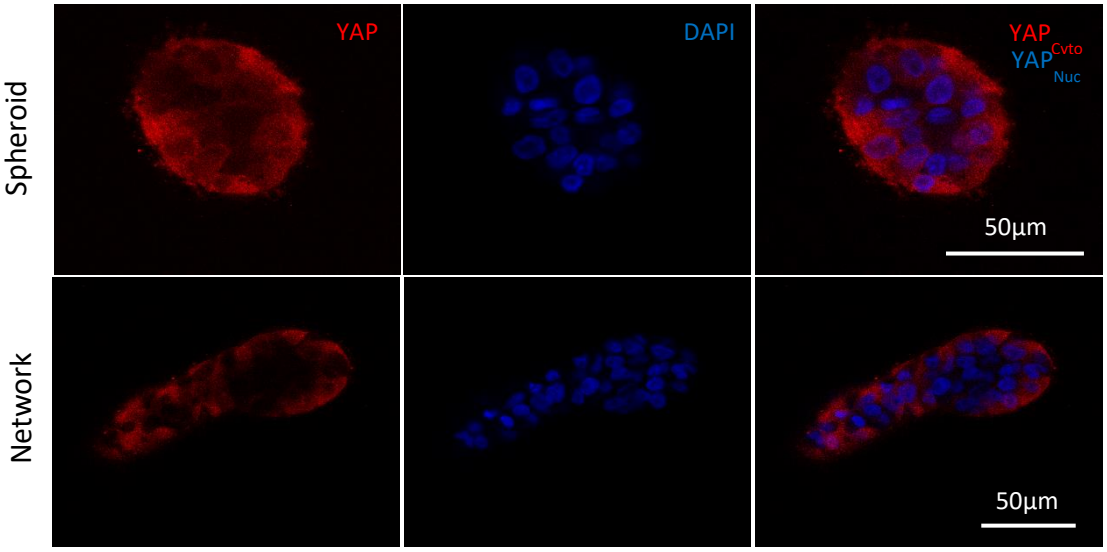

Figure 5. Confocal images of YAP expression in MDA structures. Representative images of spheroid and network phenotypes. Individual cell YAP expression appears to be heterogeneous and higher around the perimeter of structures.

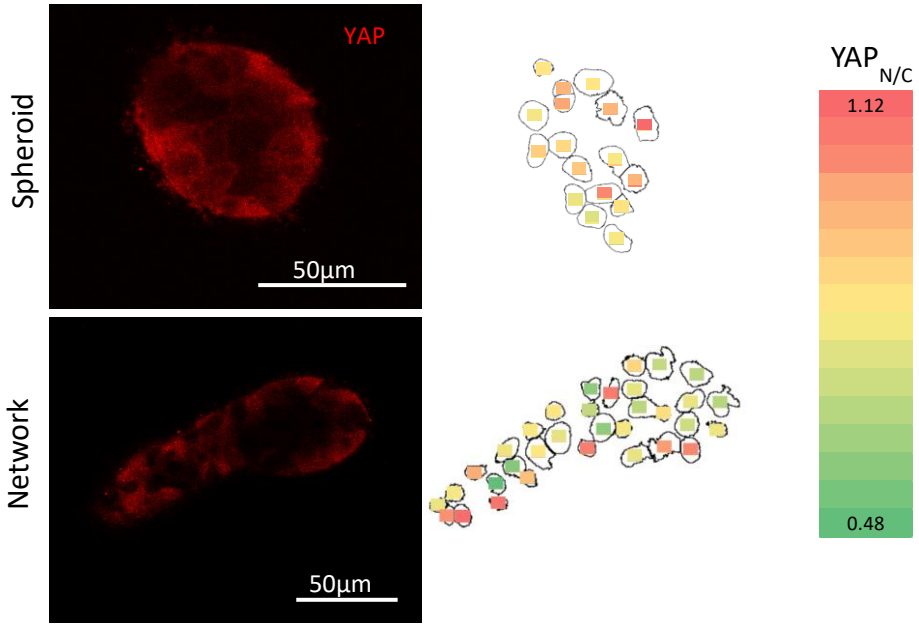

Figure 6. MDA structures do not display spatial organization of $YAP_{N/C}$ at day 7. Individual cell $YAP_{N/C}$ in non-invasive (spheroid) and invasive phenotypes (network). Higher $YAP_{N/C}$ does not occur in cells at the structure perimeter.

3.2.4. The Importance of Contractility in Cell Structures

In Carey et al. inhibition of contractility rescued the invasive phenotype in floated hydrogel structures by destabilizing cell-cell adhesions. [5] I hypothesized that if cell-cell adhesion is also stabilized in floated MDA and MCF10A structures, contractility inhibition should produce a similar effect. Contractility was interrogated with several contractile machinery inhibitors including ROCK I,II inhibitor Y-27632 and myosin light chain kinase (MLCK) inhibitor ML-7. Floated structures incubated with either drug displayed extensive invasive protrusions throughout 7 days of culture. (Figure 6, 7) ROCK I, II inhibited floated structures formed abundant thin branches and often developed into hybrid phenotypes including spheroids with extensive thin branching. (Figure 6) MDA cells incubated with the myosin light chain kinase inhibitor in general retained more stable network and spheroid phenotypes despite having thin protrusions. (Figure 7) This suggests that different regulators of the contractile signaling pathway influence different parts of development and growth.

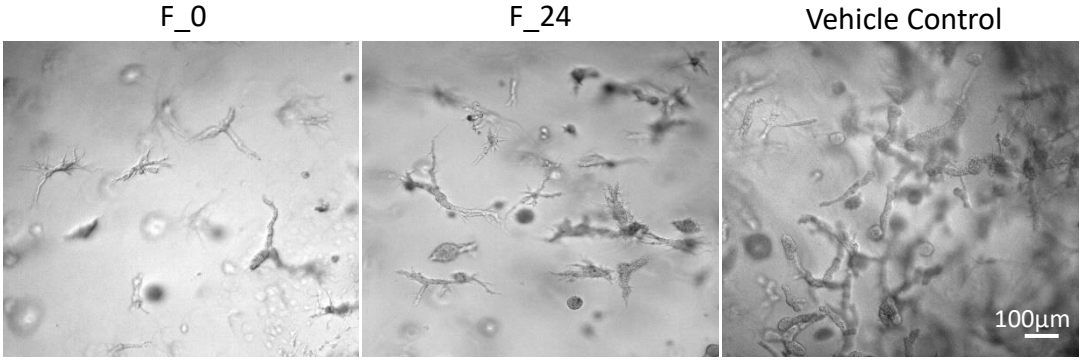

Figure 7. Brightfield Images of floated hydrogel MDA cells treated 10µM Y27632 ROCK I, II inhibitor during development. Comparison of floated hydrogel conditions treated with 10µM Y27632 ROCK I, II inhibitor to a vehicle control. Images were taken at day 7.

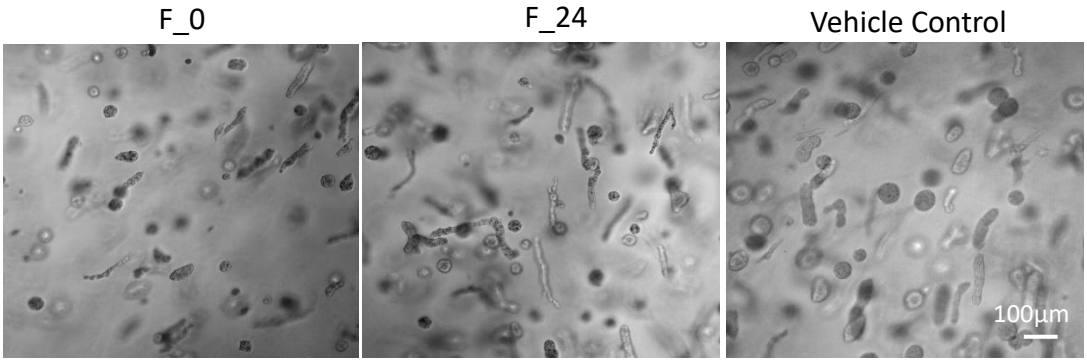

Figure 8. Brightfield Images of floated hydrogel MDA cells treated 20µM ML-7 MLCK inhibitor during development. Comparison of floated hydrogel conditions treated with 20µM ML-7 MLCK inhibitor to a vehicle control. Images were taken at day 7.

In addition to the extensive protrusions observed, cell count within inhibited floated structures was significantly less than the floated vehicle control. (Graphs 18-21) Taken together with our previous results on pFAK, this suggests that contractile tension and cell-cell adhesion can suppress invasive and promote proliferative characteristics in cancer cells.

Graph 18. Floated hydrogel MDA cells treated 10μM Y27632 ROCK I, II inhibitor during development have significantly decreased network structure cell counts. Comparison of floated hydrogel networks treated with 10μM Y27632 ROCK I, II inhibitor to a floated vehicle control treated networks. Statistical significance is tested by ANOVA and reported as p<0.001, ***; p<0.01, **; p<0.05, *.

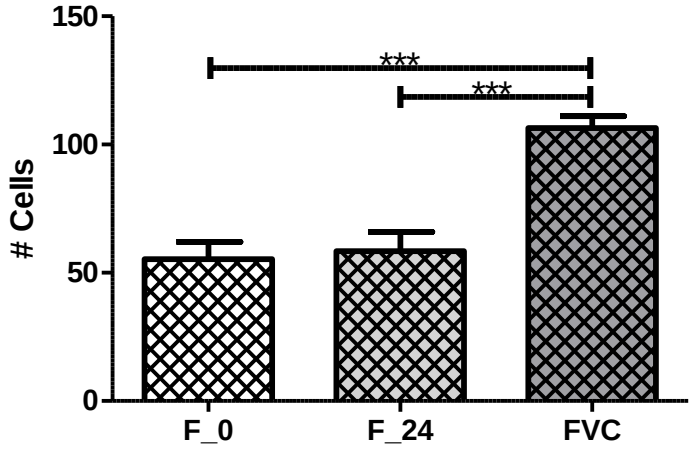

Graph 19. Floated hydrogel MDA cells treated 10μM Y27632 ROCK I, II inhibitor during development have significantly decreased spheroid structure cell counts. Comparison of floated hydrogel spheroids treated with 10μM Y27632 ROCK I, II inhibitor to a floated vehicle control treated spheroids. Statistical significance is tested by ANOVA and reported as p<0.001, ***; p<0.01, **; p<0.05, *.

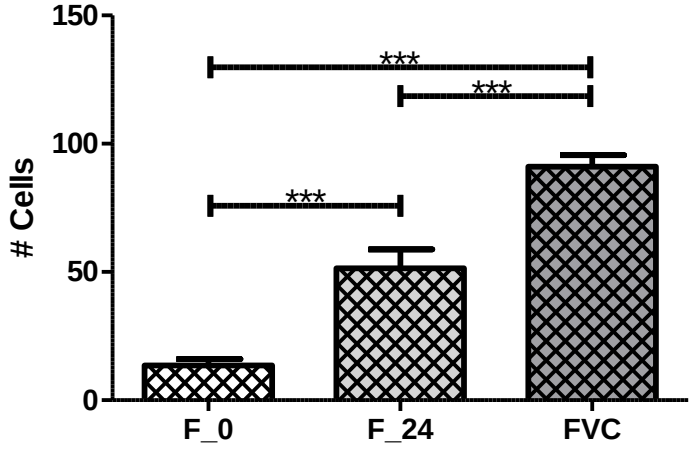

Graph 20. Floated hydrogel MDA cells treated 20μM ML-7 MLCK inhibitor during development have significantly decreased network structure cell counts. Comparison of floated hydrogel networks treated with 20μM ML-7 MLCK inhibitor to a floated vehicle control treated networks. Statistical significance is tested by ANOVA and reported as p<0.001, ***; p<0.01, **; p<0.05, *.

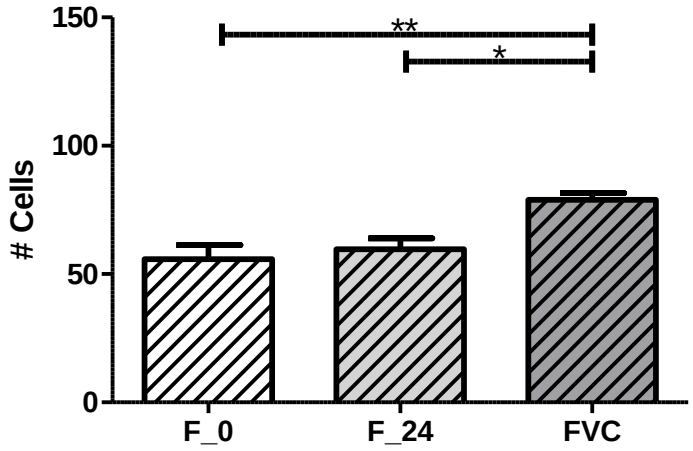

Graph 21. Floated hydrogel MDA cells treated 20μM ML-7 MLCK inhibitor during development have significantly decreased spheroid structure cell counts. Comparison of floated hydrogel spheroids treated with 20μM ML-7 MLCK inhibitor to a floated vehicle control treated spheroids. Statistical significance is tested by ANOVA and reported as p<0.001, ***; p<0.01, **; p<0.05, *.

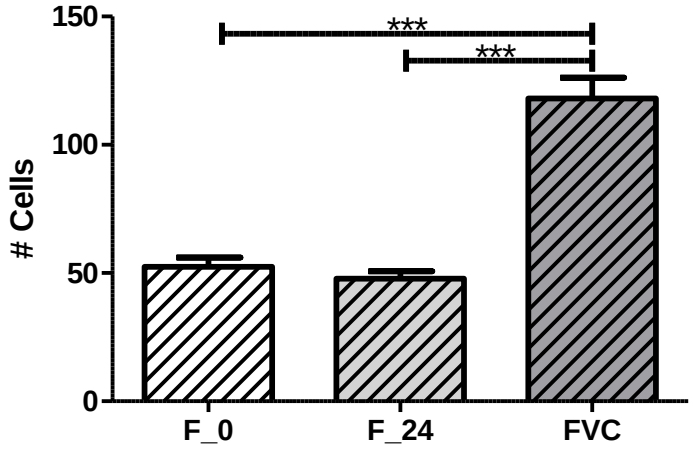

3.2.5. Calcium Mediated Cell-Cell Adhesions

The cadherin superfamily is central to cell-cell adhesion in both non-invasive and invasive cells. It has been heavily implicated in tension mediated signaling between cells including roles in regulating contact inhibition of proliferation (CIP) and locomotion (CIL) in normal cells as well as supporting collective invasion in cancer cells. Given the pseudo-normal morphology displayed by breast cancer cells in floated structures, I hypothesized that E-cadherin (ECAD) expression would be more localized to cell-cell contacts in these conditions. Immunostaining for ECAD demonstrated diffuse mainly cytoplasmic expression, which did not localize to cell junctions. (Figure 8)

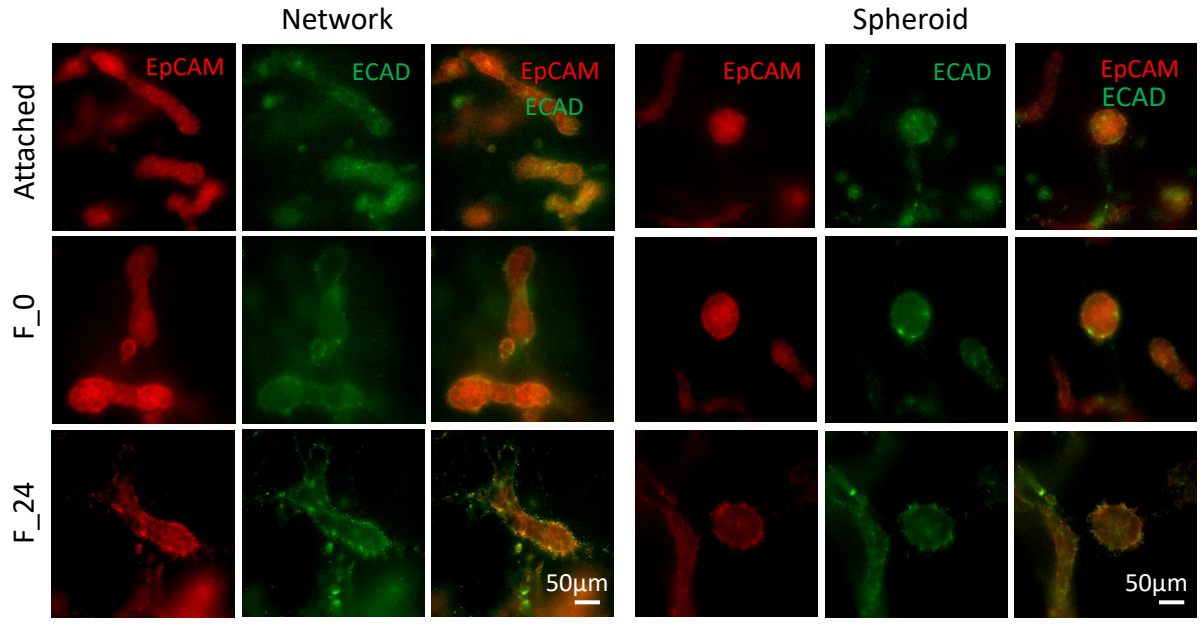

Figure 8. Confocal images of ECAD localization to cell-cell contacts in MDA structures in attached and floated hydrogel conditions. EpCAM serves as the membrane stain. ECAD does not demonstrate consistent localization at cell-cell membrane interfaces (cell-cell contacts). ECAD expression is mostly cytoplasmic and disperse.

When I repeated this experiment with more normal MCF10A cells, which form very similar structures, distinct ECAD localization occurred at cell contacts. (Figure 9) This suggests that MDA cells may employ another cadherin protein to regulate cell-cell adhesion.

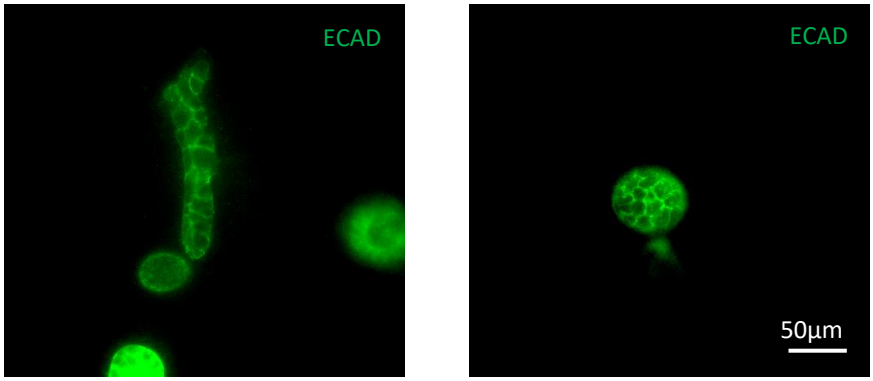

Figure 9. Confocal images of ECAD localization to cell-cell contacts in MCF10A structures in the attached hydrogel condition. ECAD expression is strongly localized.

To support this idea, I incubated MDA structures with 2-4uM EDTA, a calcium chelator to disrupt calcium mediated cell contacts. In line with previous studies, I noticed loosening of cell-cell contacts within structures (Figure 10), which was recoverable with washing and incubation in fresh media. [12,13] Disruption of cell contacts indicated calcium mediated adhesion plays an important role in MDA structure stability. Although we did not identify the primary cell-cell adhesion protein governing MDA structure development, our functional evidence justifies the importance of future experiments to address this question.

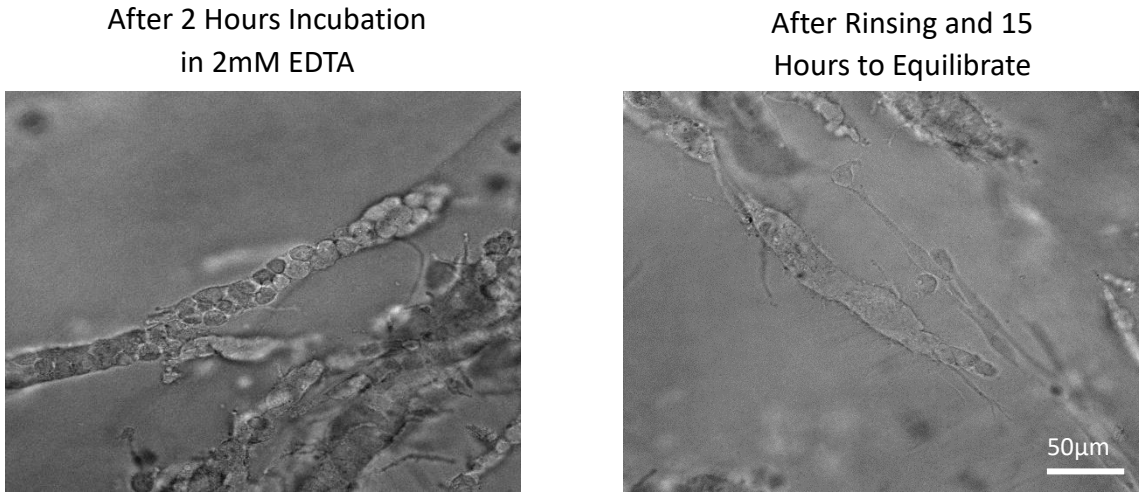

Figure 10. Brightfield images of cell-cell contact loosening in an MDA network treated with 2mM EDTA. Treatment for 2hrs at 37°C.

CHAPTER 4: DISCUSSION

Cancer metastasis is a complex process by which a subpopulation of cells in the primary tumor are stimulated to migrate out of the current tissue, traverse through several completely new environments and evade immune detection on the way to a distant part of the body. To understand how and why this possibly occurs, we need to understand how cancer senses its environment and how the environment, including adjacent cells, influence cancer cell behavior. Appreciation of normal cell behavior and its regulators is paramount to better understanding cancer since it demonstrates proficiency in hijacking and dysregulating normal cell processes. There is also evidence that cancer retains memory of its unmutated lineage, and experiments have demonstrated the cancer can readopt pseudo normal behavior when placed in non-aberrant environments. In this study we compared the invasive characteristics of normal and cancer cells in low tension environments. As previously shown, reduction of the invasive phenotype was demonstrated in both cell types, however there was also development of pseudonormal phenotypic features as well as a unique increase in proliferation among floated hydrogel collectively migrating structures. In light of these unexpected observations, I wanted to understand how low tension could prompt change in morphological development and distinct changes in cell count within structures.

4.1. Analysis of the Model

From the evidence gathered in my study, I hypothesize that release of matrix tension reduces the amount of force cells must balance with the ECM (i.e. from polymer shrinkage during polymerization and the contribution from individual cell matrix contractions), much like if a rubber band initially held taut, was then released from one end. Consequently, cells, much like the rubber band, now have additional elastic potential to distribute among multiple cell-cell contacts. (See Figure 11-12) Previous work with our MDA cells as well as reports in the literature using other breast cancer cell lines demonstrated that inhibition of important cell-ECM

adhesion protein ITGB1 promoted a near homogeneous formation of the non invasive spheroid phenotype. [21,25] Therefore, ITGB1 expression may be reduced in low tension hydrogels. Yasuda, et al. demonstrated that in cell aggregation experiments, ITGB1 expression can be negatively correlated with ICAM-1 expression, a cell-cell adhesion protein we have previously identified as upregulated in our attached day 7 gels. [26,20] This relationship suggests one possible theory of how reduced ITGB1 expression could help modulate increased aggregation and set the stage for additional cell-cell mediated increases in proliferation. Since calcium chelation disrupted cell-cell adhesion and MCF10A structures demonstrated highly localized ECAD staining at cell borders, calcium mediated AJs were examined to identify possible ways it could promote proliferation.

Based on the hypothesis that ITGB1 expression may be reduced and the observation that nascent ECM deposition remained the same in floated hydrogel structures, the increased pFAK expression observed is more likely be associated with AJs. FAK proteins have been shown in literature to be recruited to alpha and beta catenin proteins at the site of AJs, providing a possible method by which cell-cell adhesions could mediate downstream proliferative behavior. [27,28] Additionally, tension at AJ has been demonstrated by literature to stimulate inhibition of the HIPPO pathway, which promotes downstream proliferation and morphogenesis. [29,26] Despite the cancer cells undergoing increased proliferation, floated hydrogel structures retain the two major phenotypes and furthermore develop pseudo-normal organization, suggesting cancer cells display greater memory of their unmutated cell lineage. Greater regulation of the HIPPO pathway by floated hydrogel structures could help control development of the floated phenotype, however it would be naive to think one pathway is sufficient for control.

Finally, evidence of partial lumen patency in networks and spheroids suggest that in conjunction with supportive ECM deposition (COL4A1 and LAMC2), a proper balance of cell-cell and cell-ECM tension is achieved in floated hydrogels structures. Overall, the model provides a

working hypothesis of how the low tension environment may induce less invasive and more proliferative phenotypic characteristics. Substantial validation of the current model's proposed connections and exploration into other potential pathway connections will be needed to better understand the effect of low tension on collectively invading structures.

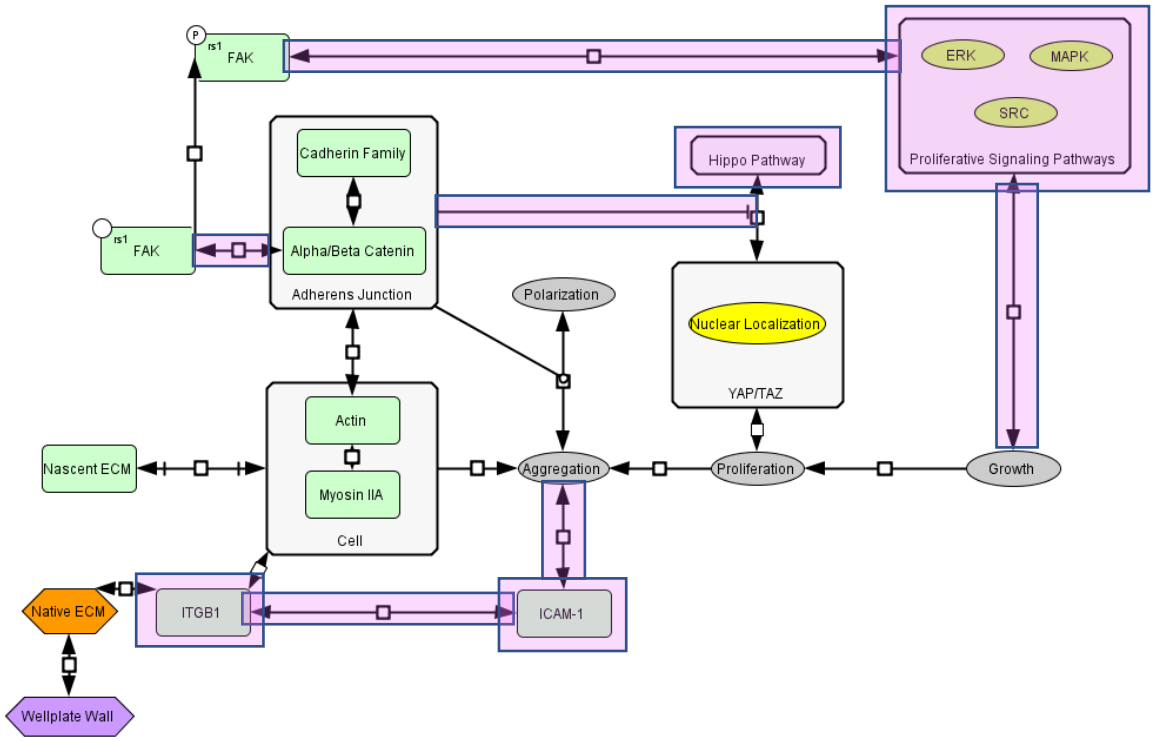

Figure 11. Proposed Model: Attached Condition. Native ECM node is attached to well plate node, indicating that tension actively exists in hydrogel. Purple outline indicates hypothesized interactions.

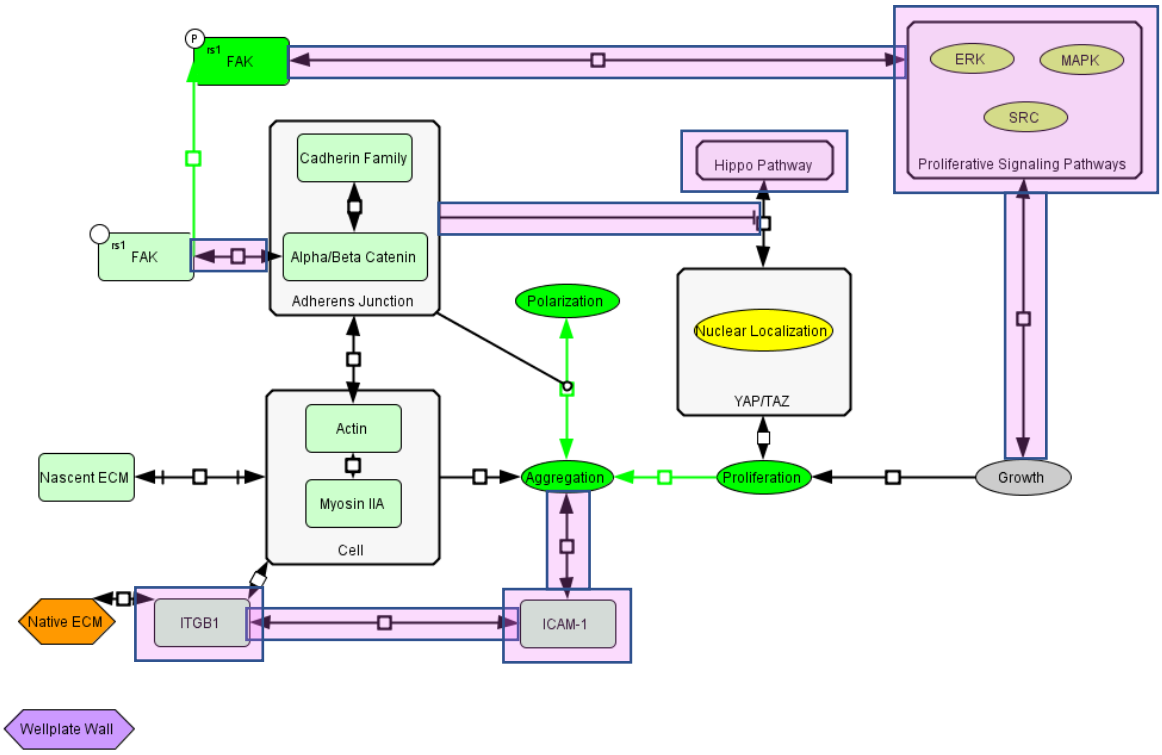

Figure 12. Proposed Model: Floated Condition. Native ECM node is detached from well plate node, indicating that tension has been released in hydrogel. Purple outline indicates hypothesized interactions. Bright green indicates upregulated molecules or pathways.

4.2. The Effect of Microenvironment and Cell Invasive Potential on Phenotype Shift

Many studies compare the effect of drug treatment on invasive cancer cells, non invasive cancer cells, and sometimes also a related normal cell line, but few studies appreciate the invasive potential of the cell microenvironment used. [30,31,32] In our study, we looked at a non invasive normal cell line and an invasive cancer cell line within up to 2 environments of different invasive potential. Using the attached hydrogel as a baseline, HD hydrogels produced a higher percentage of invasive MDA structures as compared to LDSF. As evident by the phenotype distribution shift with release of matrix tension, I observed that normal cells in less invasive promoting hydrogel environment (LDSF) experienced the greatest fold change in phenotype

shift to the non invasive phenotype. Meanwhile, more invasive MDA cancer cells in the HD environment demonstrated the smallest fold change in phenotype shift. Initial invasive potential appears to regulate the effect of floatation on phenotype shift. This suggests in future treatments using tension release, phenotype shift potential may be more favorable for an early disease prognosis where both the environment and cell of interest is less aberrant. However, it is also important to understand the effect of the nascent environment deposited by cells in response to their environment. As the bridge between cell and the native ECM microenvironment, nascent ECM deposition is also an important factor to monitor in experiment development.

4.3. Perspective on ECM deposition and Indicators of Phenotypic Reversion (PR)

Nascent ECM expression was observed and used as an indicator of cell-ECM interaction between different hydrogel conditions. We did not identify any biologically relevant differences in ECM thickness between different hydrogel conditions, but also no difference between invasive or non invasive structure types at day 7. The “go or grow” hypothesis would suggest that invasive structures would not need to lay down nascent ECM for proliferative stability, yet they do. A “go and grow” dynamic may be supported by heterogeneous cell functions within collectively migrating structures. If instead nascent ECM deposition was overexpressed in collectively migrating cancer cells irrespective of invasive phenotype, we could then hypothesize that the less invasive structure by virtue of remaining in the same location, should have greater nascent ECM thickness, yet our data suggests it does not. These observations may suggest that collectively migrating cancer cells can regulate their nascent ECM production.

Fluctuation in ECM deposition has been previously indicated in normal mammary TLDU extension. Previous literature in mammary development had indicated that bulb end regions displayed lower thickness deposition in comparison to the neck (body) regions during periods of directed invasion into the mammary fat pad. These regions of lower deposition had been predicted to work in conjunction with internal positioning of myoepithelial cells to direct extension and branching direction. [33] Greater appreciation of the temporal element in structure

development suggests the possibility that actively growing cancer structures could have had this difference in ECM deposition to guide extension, and that more mature structures (day 7) simply redistribute ECM.

Interestingly during structure development, the individual cell populations that tend to become our spheroid structures have been observed to tightly rotate around each other. This interaction has been indicated in normal acini development and coined Coherent Angular Motion (CAMo) by the Bissell lab. [34] The rotation has been shown to be important for homogenous ECM deposition around the perimeter of the structure, which is thought to be important for acini polarization and lumen formation/stability. Cancer cells have been shown to follow this development program, but only after PR which must occur within 36-48 hours of seeding or mechanical reversion (MR) which utilized mechanical stimulation rather than inhibition or stimulation of genes. [35,12] One of these PR processes involves inhibition of ITGB1, a behavior hypothesized to simulated in my floated hydrogels based on similar non invasive phenotypic distribution from previous work in our lab and elsewhere. [35] However, PR is usually described as strong reduction of proliferation (~90%) and the growth of acini-like structures similar in size to explanted primary mammary cells, on the order of 6-8 cell/structure. [35]. Re-expression of normal morphological organization including polarization, cytoskeletal organization, and homogenous ECM deposition is also desirable. A small population of the floated spheroid structures have been observed to support partial lumen patency, and a larger population displays homogenous perimeter deposition, suggesting that our cancer cell containing spheroids have the capacity to follow the CAMo development program.

Our network structures have also been observed to display noninvasive migration within the structure at later time points (i.e. day 7). This coordinated marching resembles CAMo, but is not subjected to strict rotation around a central axis. Perhaps this rotation also influences how ECM is deposited, and helps explain why we see similar ECM deposition regardless of phenotype. Greater understanding of cell coordination within structures will be needed to draw

conclusions regarding these claims. Furthermore, future experiments with proven promoters of PR would be fascinating to use in conjunction with floated hydrogels, to see if it can enhance PR.

4.4. Challenging Contact Inhibition

Another component to our understanding of invasive and non invasive structure development is its intimate interaction of cells with the surrounding matrix and adjacent cells. In 2D normal cell growth and aggregation is regulated by the principles of contact inhibition (CI). Contact inhibition of proliferation (CIP) describes an inhibition of proliferative behavior as cells reach high levels of cell-cell contact in the absence of free space to maneuver. [36] Contact inhibition of locomotion (CIL) describes, in the aftermath of a cell-cell (or object) collision, a refrain in movement in the current direction. Within a confining proximity with other cells or barriers, CIL reduces cell velocity. [37,38] These terms help describe the social behavior of normal cells in culture and in vivo. Loss of these cellular controls is a hallmark of cancer, and is vital to collective cell migration. Yet in a 3D environment, the concept of free space is less straightforward.

Our collectively migrating structures form primarily 2 phenotypes which aggregate in consistent shapes. After floatation both networks and spheroids increase in width or diameter, respectively, while the network structure undergoes further spatial organization with the development of bulbed ends. These observations seem to contradict the current theory of CIP and the lack of cancer's adherence to it, which is admittedly far more characterized in 2D models. Additionally, previous results suggest that our collectively invading network structures migrate persistently within the matrix, which suggests a lack of understanding of what is free space in 3D. As a model of metastasis, our hydrogel environment suggests that collectively invading metastasizing cells may be susceptible to some regulations of CI. Future testing and development of a refined understanding of how CI applies in 3D and in certain cancer phenotypes could provide additional tools to control and stop metastasis. Developing an

understanding of what regulates cell connection with collectively migrating structures can provide new evidence of how CI operates in 3D as well as in cancer.

CHAPTER 5: CONCLUSIONS AND FUTURE WORK

A comparison of invasive behavior among normal MCF10A breast epithelial cells and invasive MDA-MB-231 triple negative breast cancer cells demonstrated that release of tension in a COL I rich invasive environment could promote phenotypic reversion to a more non invasive phenotype in both cell types. In line with Carey et al. I was able to translate their approach on small clusters of MCF10A cells to a model of collective migration where individual structure cell counts could reach over 200 cells. MDAs experienced significant phenotypic reversion albeit less dramatic than MCF10As, suggesting cancer cells may have less sensitivity to tension release. Unexpectedly I observed significant increases in proliferation among invasive and non invasive phenotypes as well as changes in morphology reminiscent of normal mammary structures, including a small percentage of structures containing patent lumens. In my thesis work, I explored what cell interactions could prompt these changes in morphology and proliferative capacity. Although I found strong evidence to support a cell-cell adhesion driven, contraction mediated development program, many of the current theories need to be further validated and built out.

The next steps in this research should first include an elucidation of the cell-cell adhesion molecule(s) which supports the change in structure morphology and /or facilitates transmission of downstream proliferative signals. We have some evidence to suggest that calcium mediated adhesion likely plays an important role in structure adhesion, but there could also be complementary adhesion molecules working in conjunction to coordinate downstream signaling. Moreover since we observed non invasive migration of cells within structures, these cell-cell adhesions could be very dynamic and transient, making their detection and quantification time sensitive. Secondly, an exploration on how floated hydrogel structures make space for additional cells could be helpful to understand the counterintuitive observation of increased proliferation with reduced tension. I did not observe any distinct change in collagen fiber alignment, nor did I notice any obvious change in bead position after rupturing cell

membranes within structures. However, my hydrogels are typically densely populated with cell structures by the day 7 time point, suggesting possible confounding matrix manipulation and loss of true bead displacement. Seeding at lower cell densities could help identify true bead displacement. Finally, there needs to be more extensive study of the temporal cues which stimulate the divergent phenotype in floated hydrogel structures. Visual observation and proliferative staining quantification suggest a day 5 timepoint could be very useful for observing increased cell division events and structure morphology changes. Use of a fucci construct in MDAs during a timelapse could identify the most active proliferative periods as well as the duration of elevated proliferation in the event that floated hydrogel structures undergo extended elevated proliferation periods.

Overall, a more complete understanding of the low tension condition may help better inform clinicians and researchers understand how residual cancer left after tumor resections supports survival and evasion of detection in follow up examinations. Furthermore, stimulation of a less invasive phenotype after tension loss may provide a better opportunity for more complete cancer eradication in targeted treatments.

REFERENCES

1. Rosenfield, S. M. & Smith, G. H. Redirection of Human Cancer Cells upon the Interaction with the Regenerating Mouse Mammary Gland Microenvironment. *Cells* **2**, 43–56 (2013).

2. Seyfried, T. N. & Huysentruyt, L. C. On the origin of cancer metastasis. *Crit. Rev. Oncog.* **18**, 43–73 (2013).

3. Wozniak, M. A. & Chen, C. S. Mechanotransduction in development: A growing role for contractility. *Nature Reviews Molecular Cell Biology* vol. 10 34–43 (2009).

4. Cox, T. R. & Erler, J. T. Remodeling and homeostasis of the extracellular matrix: Implications for fibrotic diseases and cancer. *DMM Disease Models and Mechanisms* vol. 4 165–178 (2011).

5. Carey, S. P., Martin, K. E. & Reinhart-King, C. A. Three-dimensional collagen matrix induces a mechanosensitive invasive epithelial phenotype. *Sci. Rep.* **7**, 42088 (2017).

6. Cheung, K. J., Gabrielson, E., Werb, Z. & Ewald, A. J. Collective invasion in breast cancer requires a conserved basal epithelial program. *Cell* **155**, 1639–51 (2013).

7. Fraley, S. I., Feng, Y., Giri, A., Longmore, G. D. & Wirtz, D. Dimensional and temporal controls of three-dimensional cell migration by zyxin and binding partners. *Nat. Commun.* **3**, 719 (2012).

8. Haeger, A., Wolf, K., Zegers, M. M. & Friedl, P. Collective cell migration: Guidance principles and hierarchies. *Trends in Cell Biology* vol. 25 556–566 (2015).

9. Wei, S. C., Fattet, L., Tsai, J. H., Guo, Y., Pai, V. H., Majeski, H. E., Chen, A. C., Sah, R. L., Taylor, S. S., Engler, A. J., Yang, J. Matrix stiffness drives epithelial-mesenchymal transition and tumour metastasis through a TWIST1-G3BP2 mechanotransduction pathway. *Nat. Cell Biol.* **17**, 678–688 (2015).

10. Tusan, C. G., Man, Y. H., Zarkoob, H., Johnston, D. A., Andriotis, O. G., Thurner, P. J., Yang, S., Sander, E. A., Gentleman, E., Sengers, B. G., Evans, N. D., Collective Cell Behavior in Mechanosensing of Substrate Thickness. *Biophys. J.* **114**, 2743–2755 (2018).

11. Provenzano, P. P. & Keely, P. J. Mechanical signaling through the cytoskeleton regulates cell proliferation by coordinated focal adhesion and Rho GTPase signaling. *J. Cell Sci.* **124**, 1195–205 (2011).

12. Hartsock, A. & Nelson, W. J. Adherens and tight junctions: structure, function and connections to the actin cytoskeleton. *Biochim. Biophys. Acta* **1778**, 660–9 (2008).

13. Inman, J. L. & Bissell, M. J. Apical polarity in three-dimensional culture systems: where to now? *J. Biol.* **9**, 2 (2010).

14. Marchevsky, A. M., Gupta, R. & Balzer, B. Diagnosis of metastatic neoplasms: A clinicopathologic and morphologic approach. *Archives of Pathology and Laboratory Medicine* vol. 134 194–206 (2010).

15. Hammar, S. P. Metastatic adenocarcinoma of unknown primary origin. *Hum. Pathol.* **29**, 1393–1402 (1998).

16. Adams, C. L., Chen, Y. T., Smith, S. J. & Nelson, W. J. Mechanisms of epithelial cell-cell

adhesion and cell compaction revealed by high-resolution tracking of E-cadherin-green fluorescent protein. *J. Cell Biol.* **142**, 1105–1119 (1998).

17. Furukawa, M., Wheeler, S., Clark, A. M. & Wells, A. Lung epithelial cells induce both phenotype alteration and senescence in breast cancer cells. *PLoS One* **10**, (2015).

18. Ricca, B. L., Venugopalan, G., Furuta, S., Tanner, K., Orellana, W. A., Reber, C. D., Brownfield, D. G., Bissell, M. J., Fletcher, D. A. Transient external force induces phenotypic reversion of malignant epithelial structures via nitric oxide signaling. *Elife* **7**, (2018).

19. Young, L., Sung, J. & Masters, J. R. Detection of mycoplasma in cell cultures. *Nat. Protoc.* **5**, 929–934 (2010).

20. Ranamukhaarachchi, S. K., Modi, R. N., Han, A., Velez, D. O., Kumar, A., Engler, A. J., Fraley, S. I. Macromolecular crowding tunes 3D collagen architecture and cell morphogenesis. *Biomater. Sci.* **7**, 618–633 (2019).

21. Velez, D. O., Tsui, B., Goshia, T., Chute, C. L., Han, A., Carter, H., Fraley, S. I. 3D collagen architecture induces a conserved migratory and transcriptional response linked to vasculogenic mimicry. *Nat. Commun.* **8**, 1651 (2017).

22. Mitra, S. K. & Schlaepfer, D. D. Integrin-regulated FAK–Src signaling in normal and cancer cells. *Curr. Opin. Cell Biol.* **18**, 516–523 (2006).

23. Mohan, A., Schlue, K. T., Kniffin, A. F., Mayer, C. R., Duke, A. A., Narayanan, V., Arsenovic, P. T., Bathula, K., Danielsson, B. E., Dumbali, S. P., Maruthamuthu, V., Conway, D. E., Spatial Proliferation of Epithelial Cells Is Regulated by E-Cadherin Force. *Biophys. J.* **115**, 853–864 (2018).

24. Mendonsa, A. M., Na, T. Y. & Gumbiner, B. M. E-cadherin in contact inhibition and cancer. *Oncogene* **37**, 4769–4780 (2018).

25. Wang, F., Weaver, V. M., Petersen, O. W., Larabell, C. A., Dedhar, S., Briand, P., Lupu, R., Bissell, M. J. Reciprocal interactions between β1-integrin and epidermal growth factor receptor in three-dimensional basement membrane breast cultures: A different perspective in epithelial biology. *Proc. Natl. Acad. Sci. U. S. A.* **95**, 14821–14826 (1998).

26. Yasuda, M., Tanaka, Y., Tamura, M., Fujii, K., Sugaya, M., So, T., Takenoyama, M., Yasumoto, K. Stimulation of β1 integrin down-regulates ICAM-1 expression and ICAM-1-dependent adhesion of lung cancer cells through focal adhesion kinase. *Cancer Res.* **61**, 2022–2030 (2001).

27. Playford, M. P., Vadali, K., Cai, X., Burridge, K. & Schaller, M. D. Focal adhesion kinase regulates cell-cell contact formation in epithelial cells via modulation of Rho. *Exp. Cell Res.* **314**, 3187–97 (2008).

28. Mui, K. L. Bae, Y. H., Gao, L., Liu, S. L., Xu, T., Radice, G. L., Chen, C. S., Assoian, R. K. N-Cadherin Induction by ECM Stiffness and FAK Overrides the Spreading Requirement for Proliferation of Vascular Smooth Muscle Cells. *Cell Rep.* **10**, 1477–1486 (2015).

29. Bae, Y. H., Mui, K. L., Hsu, B. Y., Liu, S. L., Cretu, A., Razinia, Z., Xu, T., Puré, E. A FAK-Cas-Rac-lamellipodin signaling module transduces extracellular matrix stiffness into mechanosensitive cell cycling. *Sci. Signal.* **7**, ra57 (2014).

30. Castelló-Cros, R., Khan, D. R., Simons, J., Valianou, M. & Cukierman, E. Staged stromal extracellular 3D matrices differentially regulate breast cancer cell responses through PI3K and beta1-integrins. *BMC Cancer* **9**, 94 (2009).

31. Wang, H., Lacoche, S., Huang, L., Xue, B. & Muthuswamy, S. K. Rotational motion during three-dimensional morphogenesis of mammary epithelial acini relates to laminin matrix assembly. *Proc. Natl. Acad. Sci. U. S. A.* **110**, 163–168 (2013).

32. Mah, E. J., Lefebvre, A. E. Y. T., McGahey, G. E., Yee, A. F. & Digman, M. A. Collagen density modulates triple-negative breast cancer cell metabolism through adhesion-mediated contractility. *Sci. Rep.* **8**, 17094 (2018).

33. Ewald, A. J., Brenot, A., Duong, M., Chan, B. S. & Werb, Z. Collective Epithelial Migration and Cell Rearrangements Drive Mammary Branching Morphogenesis. *Dev. Cell* **14**, 570–581 (2008).

34. Tanner, K., Mori, H., Mroue, R., Bruni-Cardoso, A. & Bissell, M. J. Coherent angular motion in the establishment of multicellular architecture of glandular tissues. *Proc. Natl. Acad. Sci. U. S. A.* **109**, 1973–1978 (2012).

35. Weaver, V. M. Petersen, O. W., Wang, F., Larabell, C. A., Briand, P., Damsky, C., Bissell, M. J. Reversion of the malignant phenotype of human breast cells in three-dimensional culture and in vivo by integrin blocking antibodies. *J. Cell Biol.* **137**, 231–245 (1997).

36. Pavel, M. Renna, M., Park, S. J., Menzies, F. M., Ricketts, T.,Füllgrabe, J., Ashkenazi, A., Frake, R. A., Lombarte, A. C., Bento, C. F., Franze, K., Rubinsztein, D. C. Contact inhibition controls cell survival and proliferation via YAP/TAZ-autophagy axis. *Nat. Commun.* **9**, 2961 (2018).

37. Emerman, J. T. & Pitelka, D. R. *Maintenance and Induction of Morphological Differentiation in Dissociated Mammary Epithelium on Floating Collagen Membranes*. *Source: In Vitro* vol. 13 https://www.jstor.org/stable/pdf/4291936.pdf?refreqid=excelsior%3A2d08d603a126cc74c7e333c0490f7399 (1977).

38. Roycroft, A. & Mayor, R. Molecular basis of contact inhibition of locomotion. *Cell. Mol. Life Sci.* **73**, 1119–30 (2016).